The Advanced Photon Source : An Introduction

Argonne National Laboratory, a U.S. Department of Energy Office of Science laboratory,
is operated by The University of Chicago.
The Advanced Photon Source is funded by the U.S. Department of Energy,
Office of Science, Office of Basic Energy Sciences.

Third-Generation X-ray Sources

Chasman

Greene

Low Beam Emittance (Chaseman-Green or DBA Lattice)

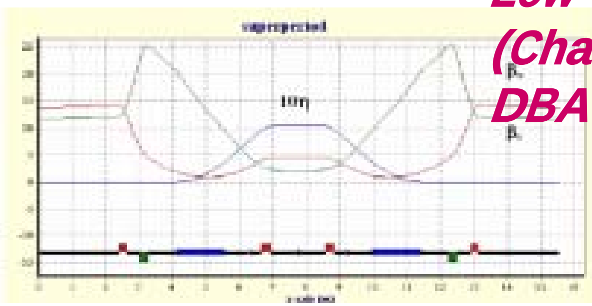

Planning Study for Advanced National Synchrotron-Radiation Facilities

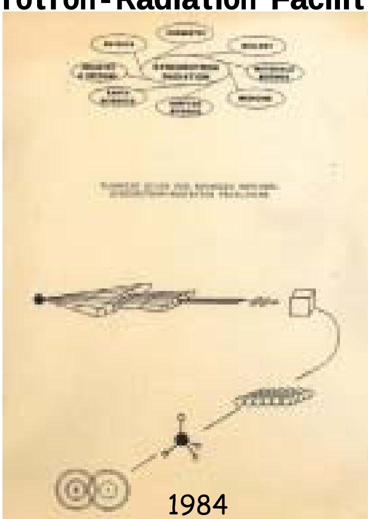

Cochairs:P. Eisenberger
M. Knotek

Scientific Drivers

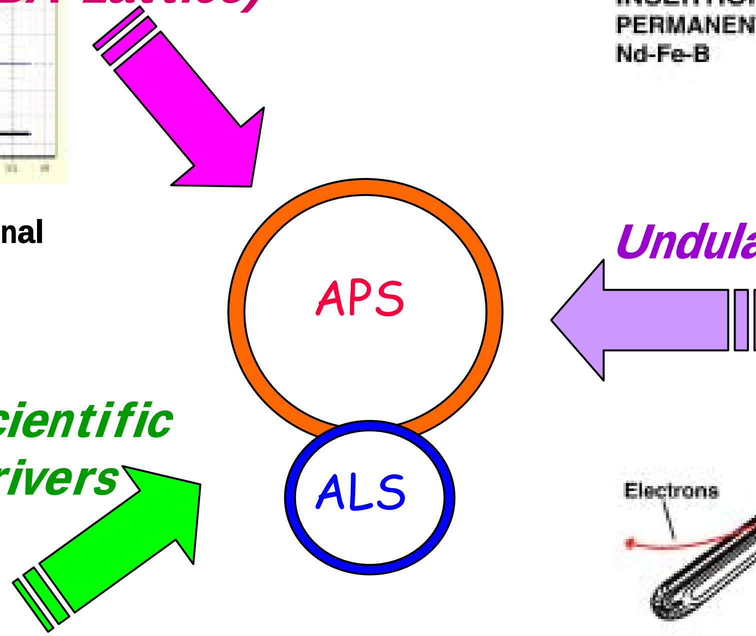

Undulator

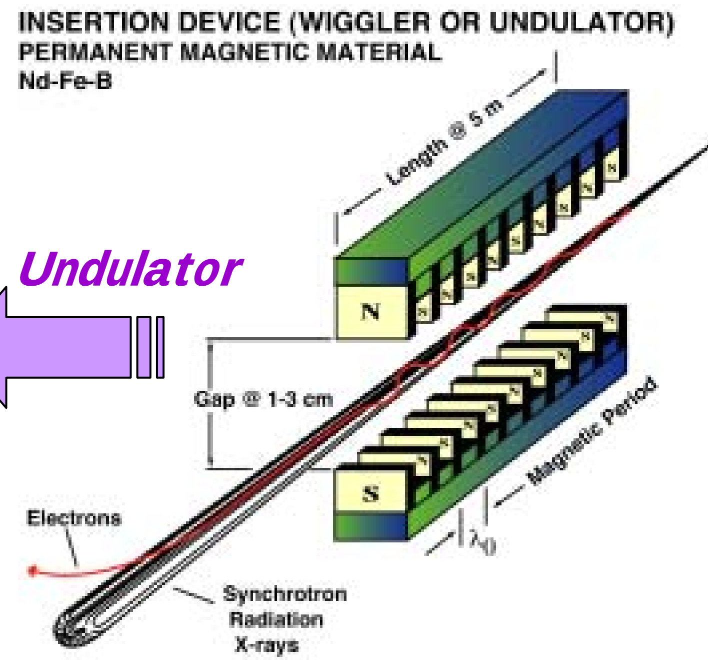

Third Generation Facilities

K. Halbach
N. Vinokurov

Science Drivers	Undulator Source
Beam Divergence ($2\sigma_x$' x $2\sigma_y$') $mrad^2$	0.001 x 0.006
Focused Beam Size, μm	< 1
Intensity in Focus, $ph/s/mm^2$	10^{14}
Sample Isodimension, μm	1-10
Sample Volume, mm^3	$10^{-3} \sim 10^{-7}$
Relative Diffraction Intensity	$10^{13} \sim 10^{9}$
Monochromatic Beam for Inelastic Scattering Ph/s/mV	$10^{9} \sim 10^{10}$
Non-Resonant Magnetic Scattered Photons/s	$10^{6} \sim 10^{7}$ /μB
Time Resolution, ph/eV/100 ps	$10^{8} \sim 10^{9}$

APS Parameters

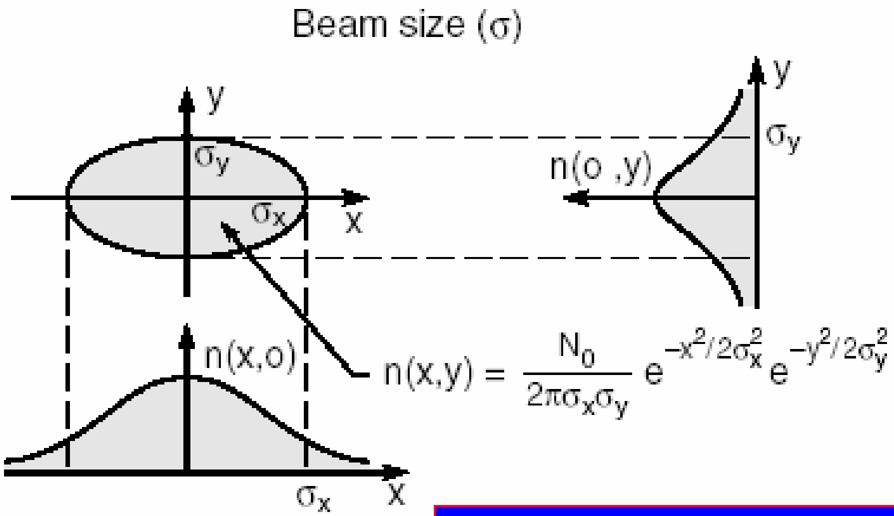

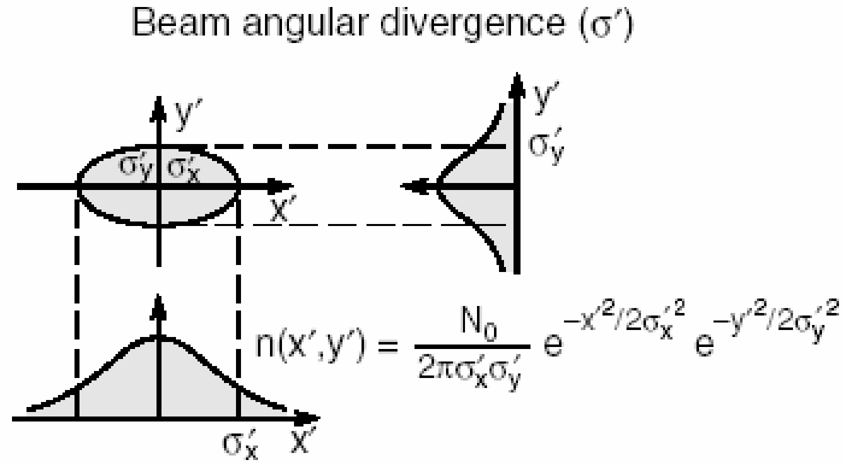

Horizontal beam size, σ_x , μm	254
Vertical beam size, σ_y, μm	12
Horizontal beam divergence, σ_x', μrad	15.6
Vertical beam divergence, σ_y', μrad	3.0

Storage ring energy, GeV	7.0
Storage ring current, mA	100
Beam energy spread, $\delta E/E$, %	0.096
Horizontal emittance, ε_x, nm-rad	3.0
Vertical emittance, ε_y, nm-rad	0.03
Coupling constant	1%
Horizontal beta function, β_x, m	14.4
Vertical beta function, β_y , m	4.0
Dispersion function, η_x, m	0.124
Orbital Priod, μs	~ 3.6

Laboratory Frame of Reference

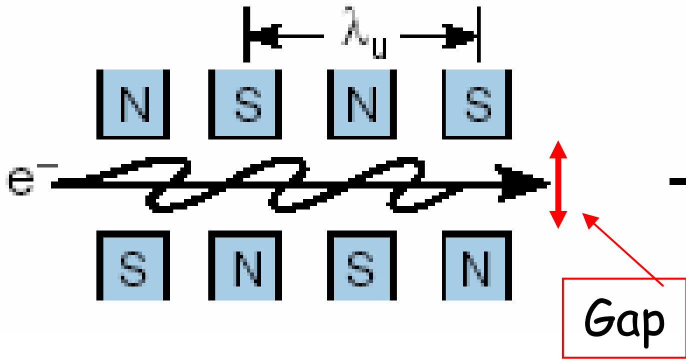

Frame of Moving e⁻

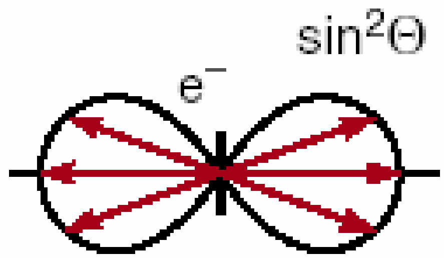

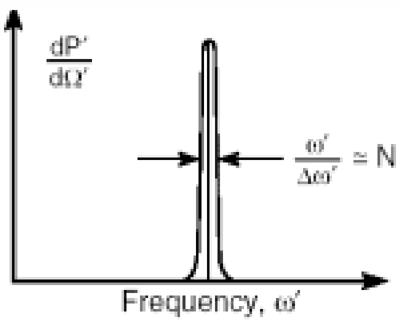

Frame of Observer

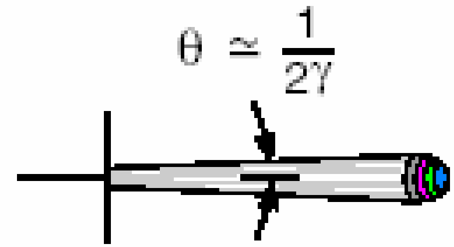

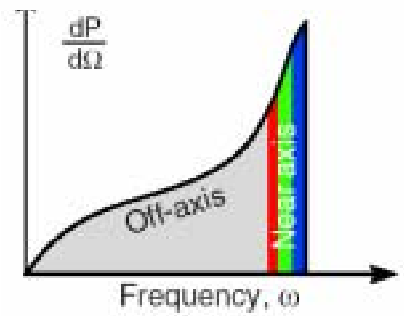

Following Monochromator

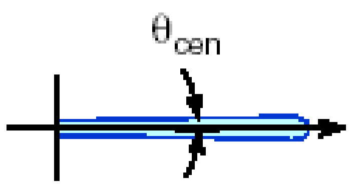

For $\frac{\Delta\lambda}{\lambda} \simeq \frac{1}{N}$

$$\theta_{cen} \simeq \frac{1}{\gamma\sqrt{N}}$$

$$\lambda = \frac{\lambda_u}{2\gamma^2}\left(1 + \frac{K^2}{2} + \gamma^2\theta^2\right)$$

$$E_n(keV) = 0.949\ E^2(GeV)\ n\ /[\ \lambda_u\ (cm)(l + K^2\ /2 + \gamma^2\theta^2)]$$

$$K = 0.934\ \lambda_u\ (cm)\ B_o(T)$$

Linac accelerating structures raise electron energy to 325 MeV

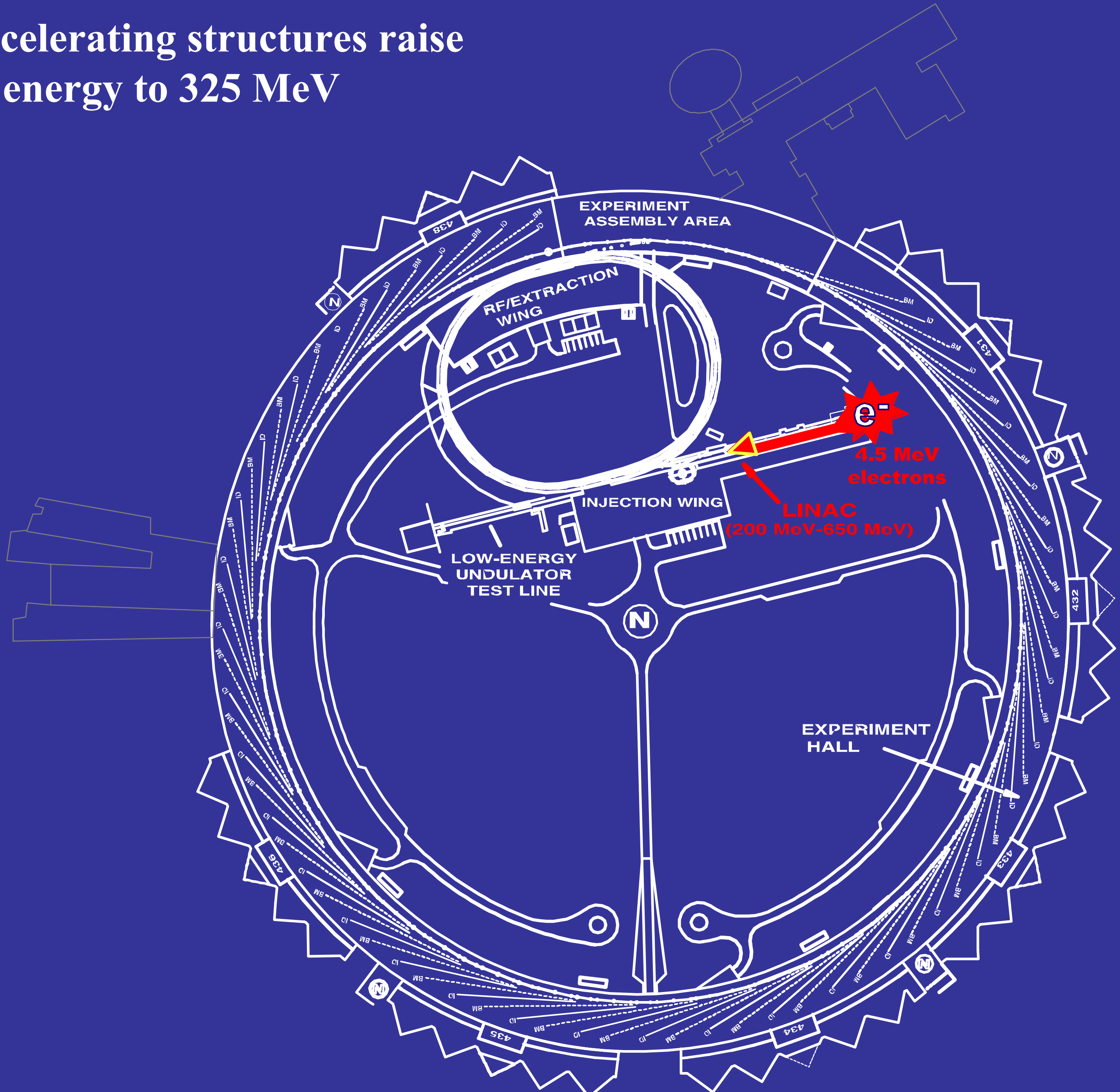

Electrons are injected into 368-m-long, racetrack-shaped booster synchrotron

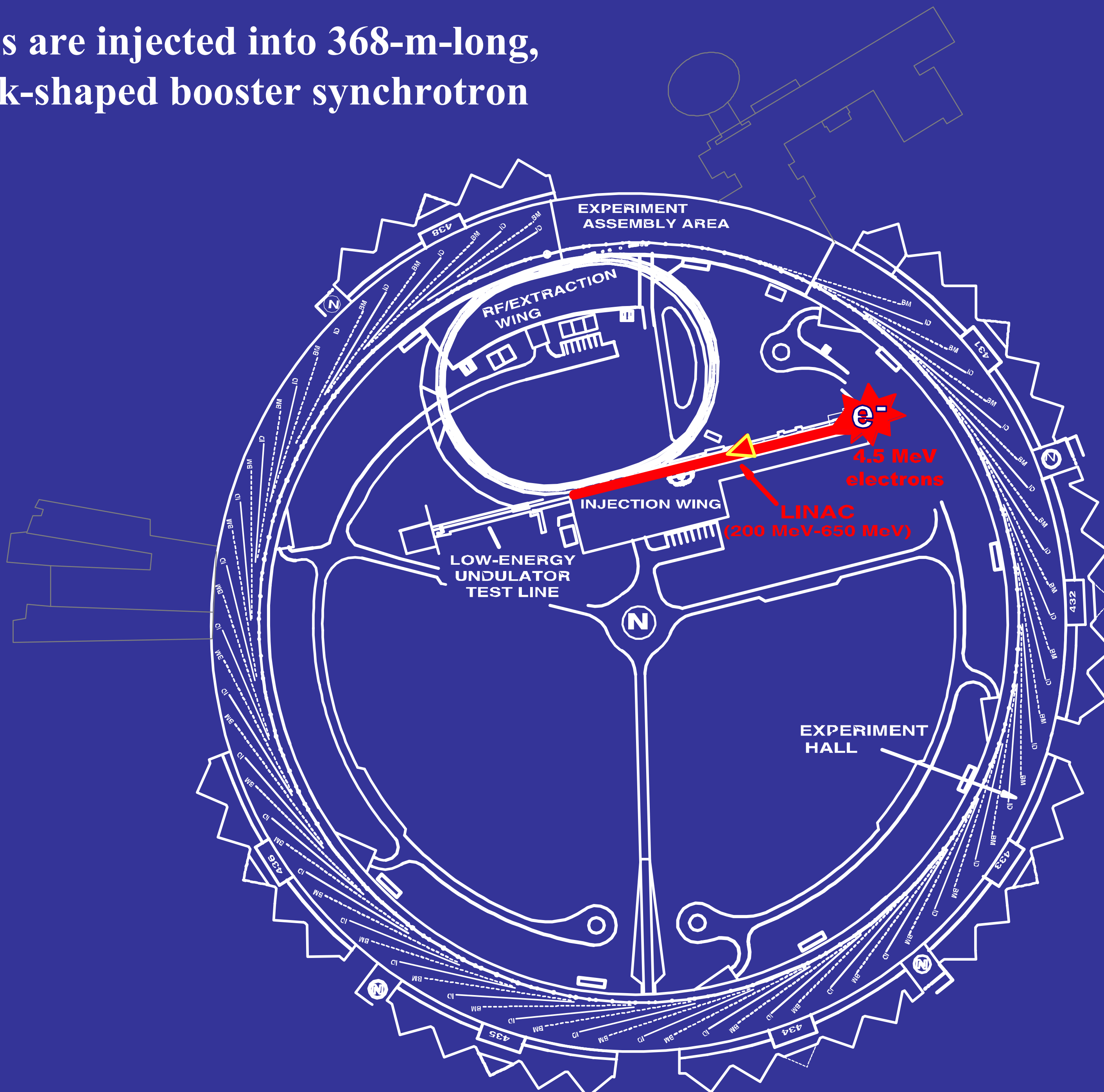

Booster raises e- energy to relativistic 7 GeV -nearly the speed of light

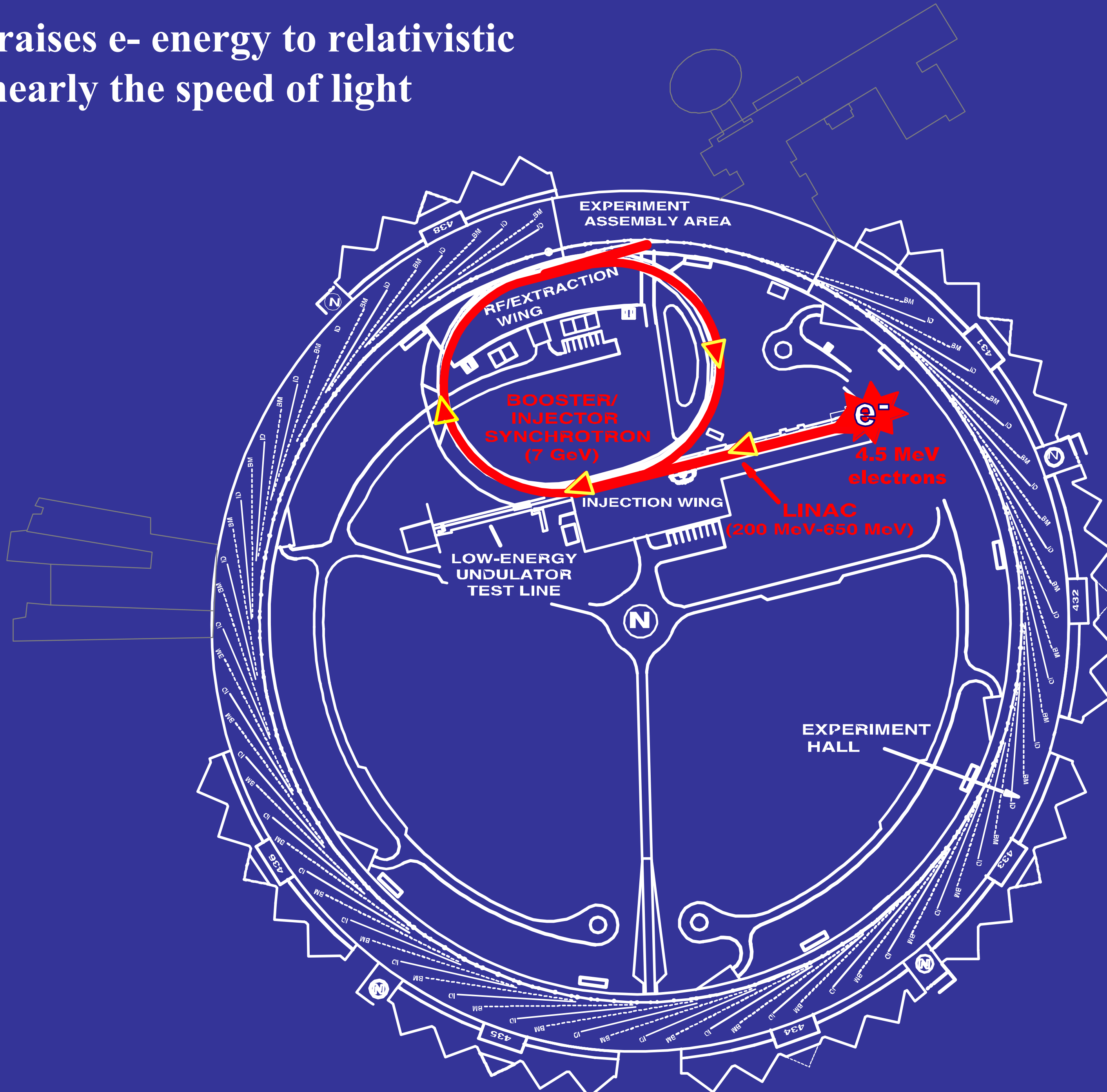

7 GeV electrons injected into 1104-m-circumference storage ring

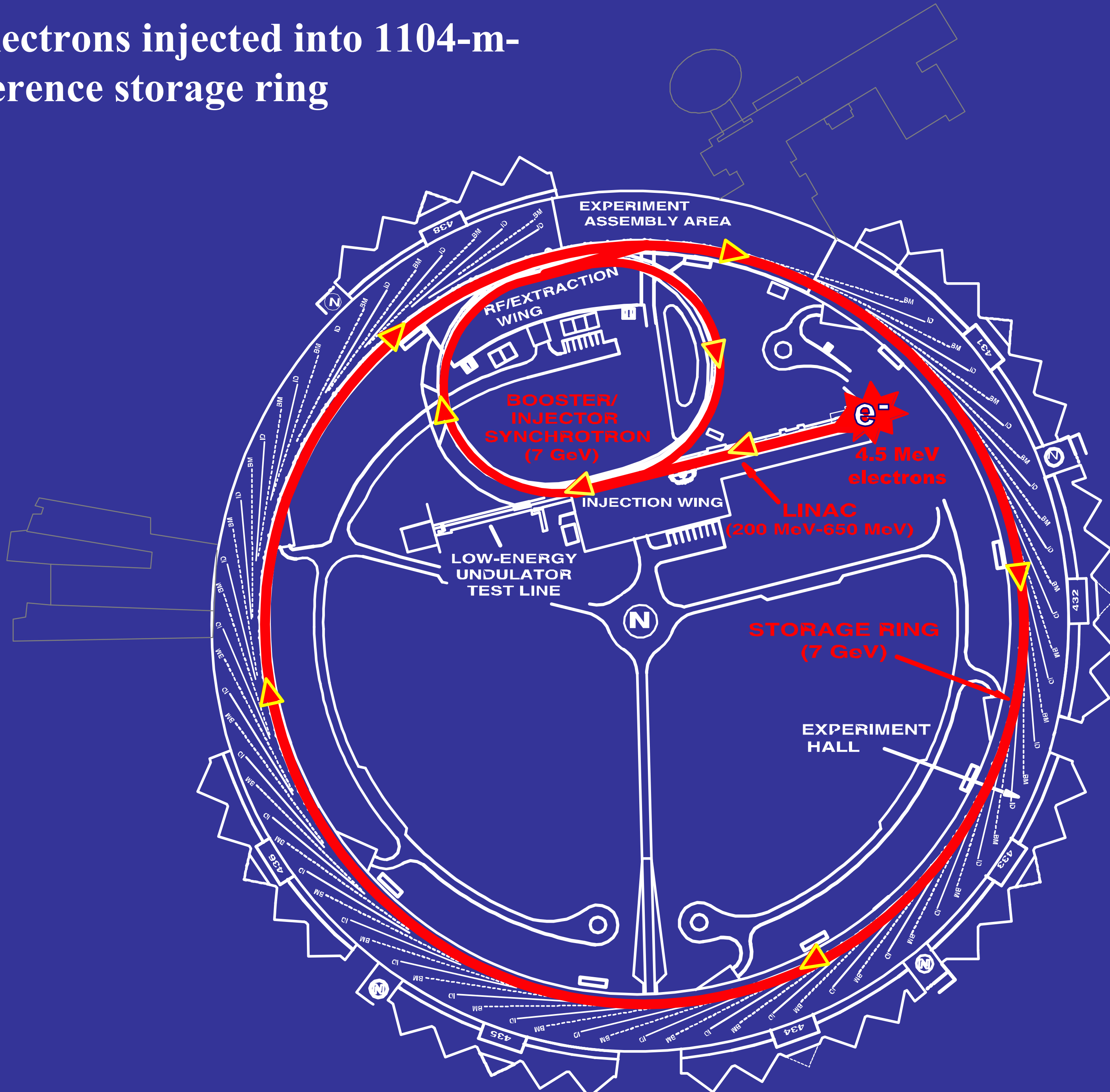

Electrons orbit for hours in storage ring, emitting synchrotron radiation from undulators….

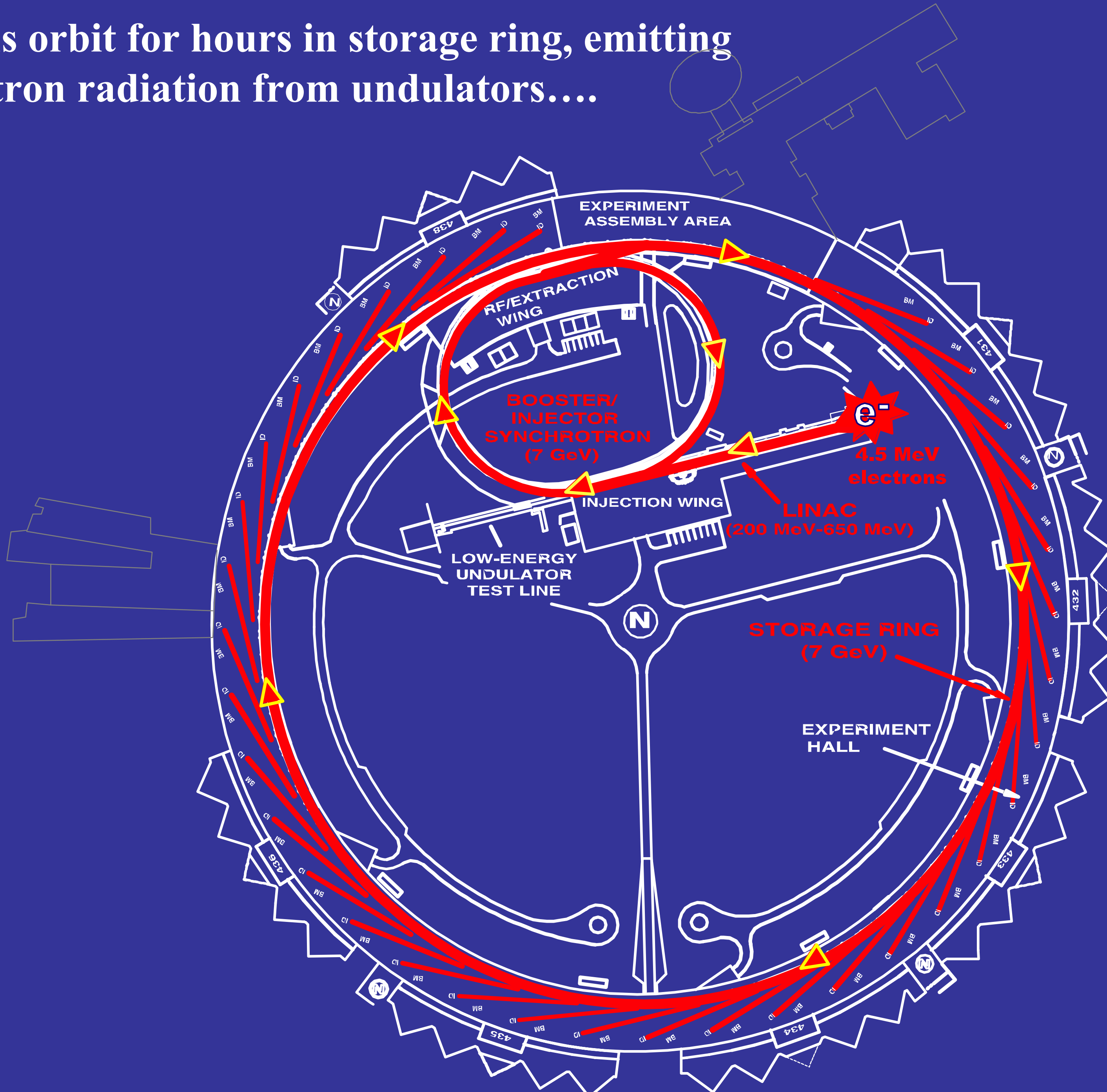

… and bending magnet beamlines

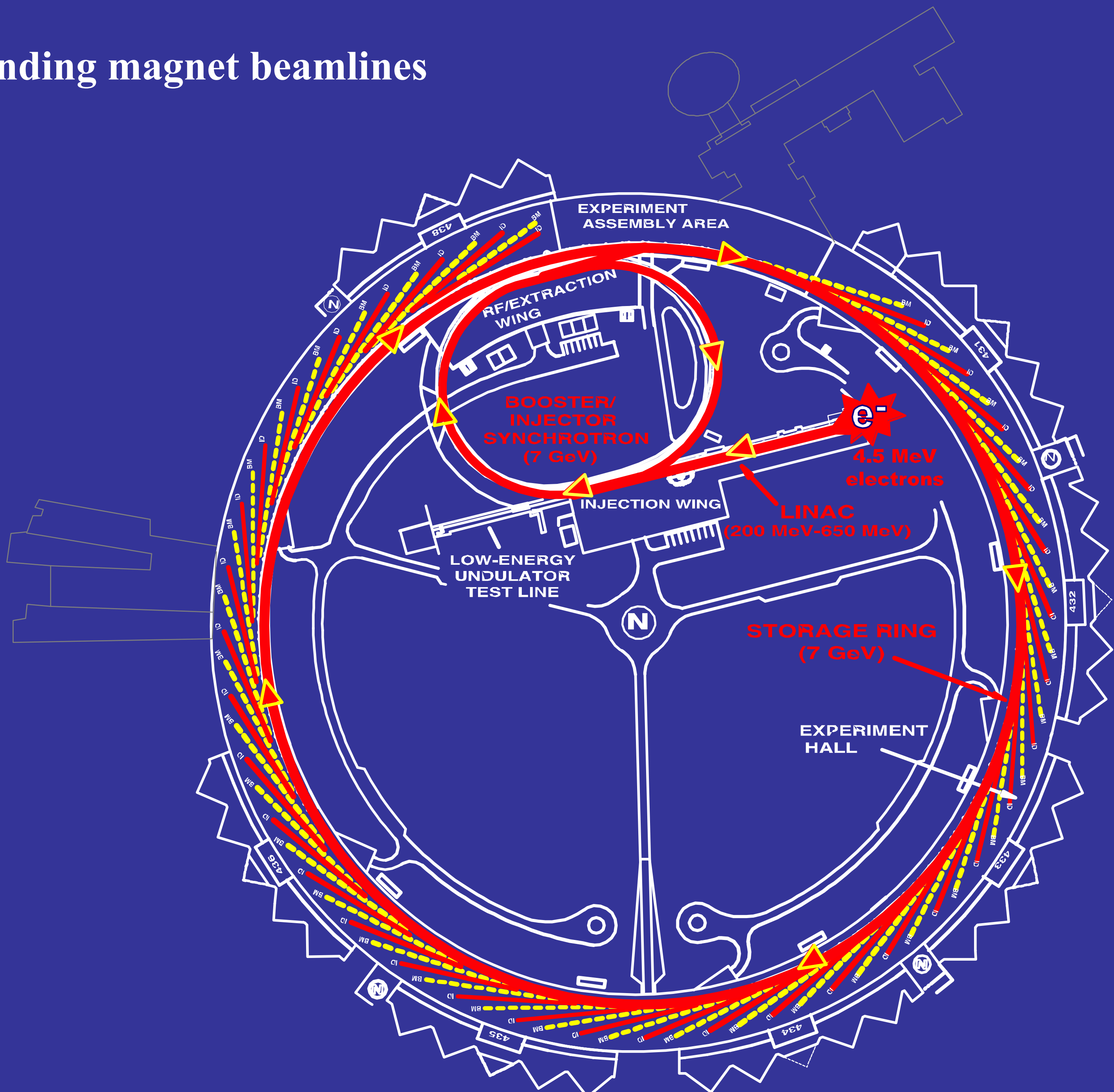

Undulator Energy Tunability

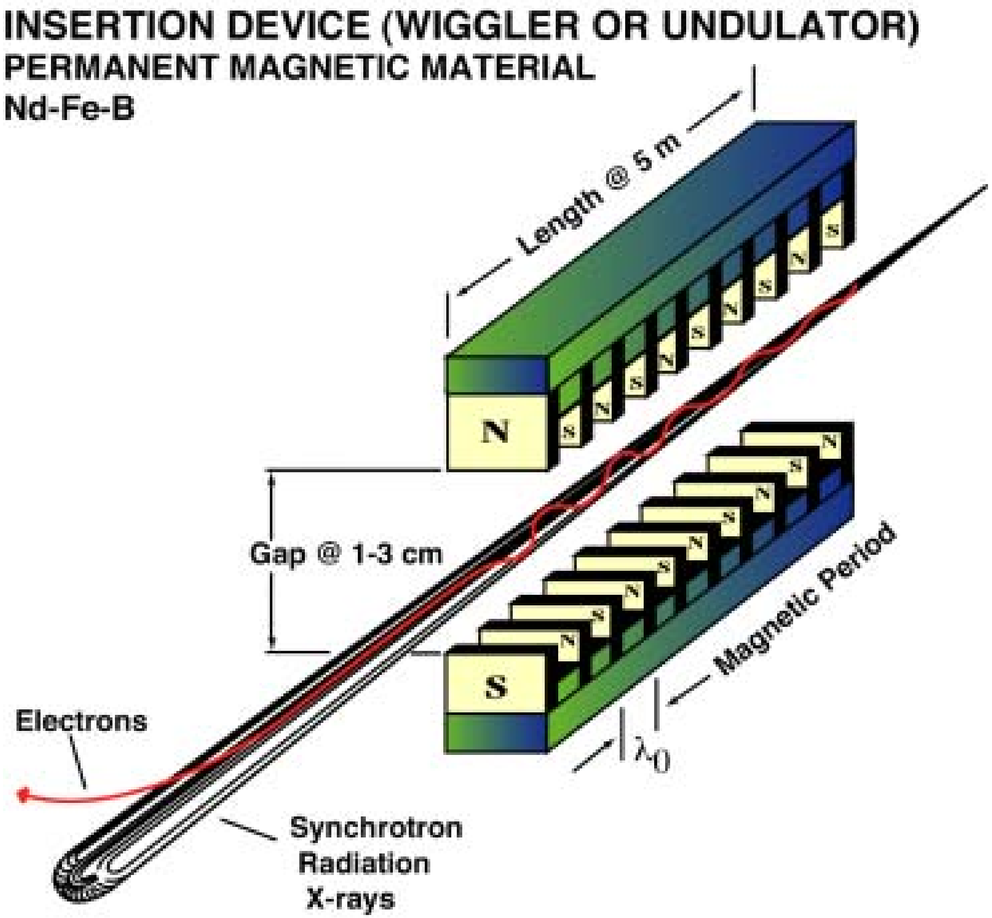

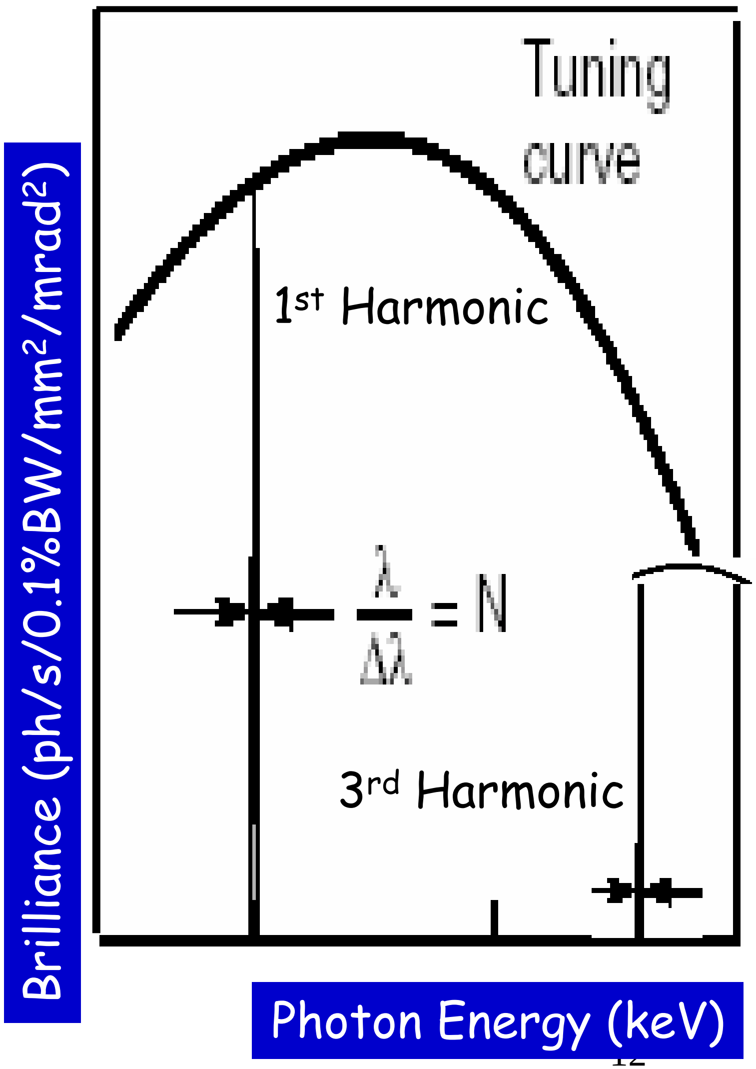

Tunability of Spectral Brightness APS Undulator A (λ_u = 3.3 cm)

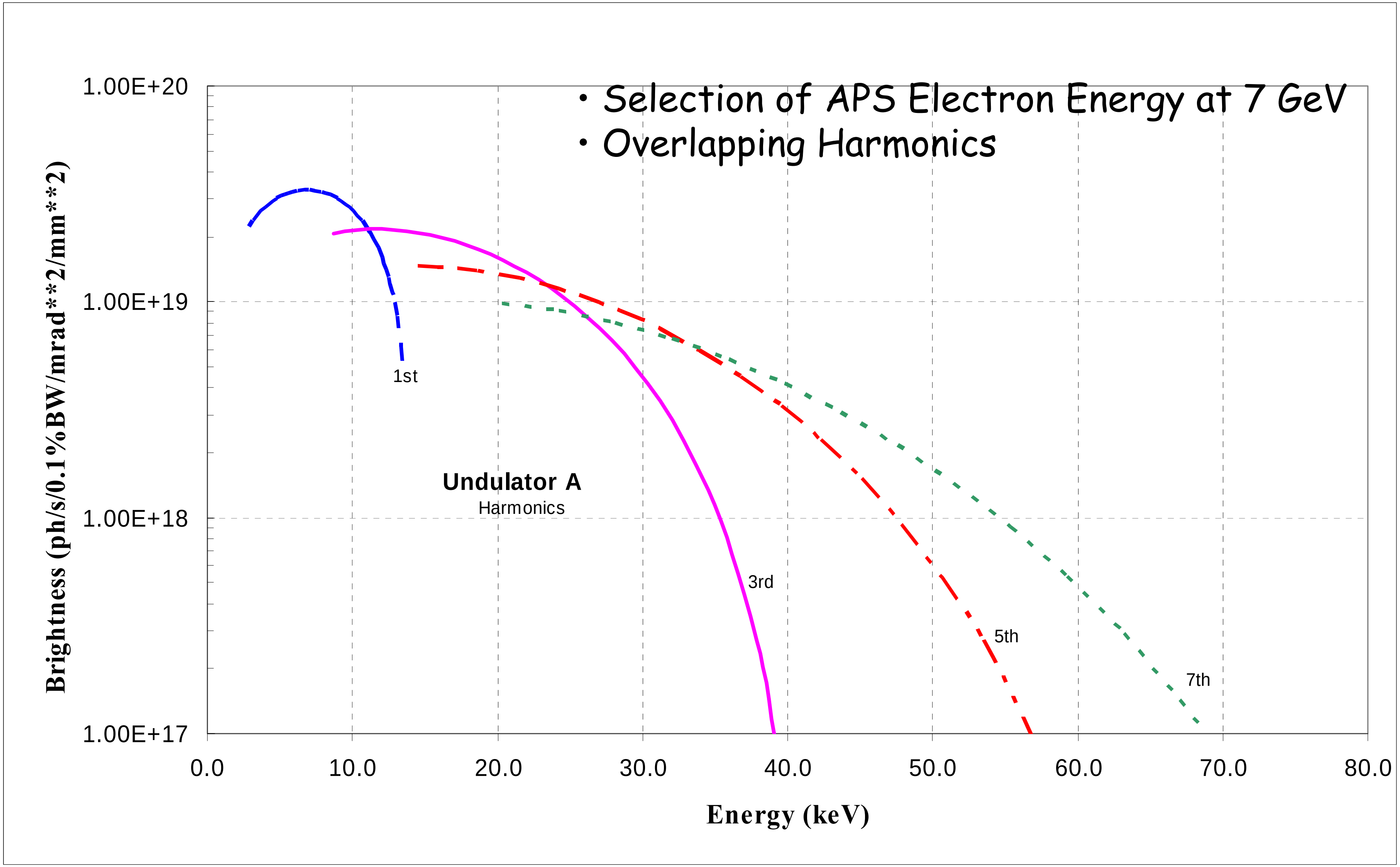

Towards Nanomagnetism of 3d, 4f and 5f Elements
Brilliance Tuning Curves for Elliptically Polarized Devices

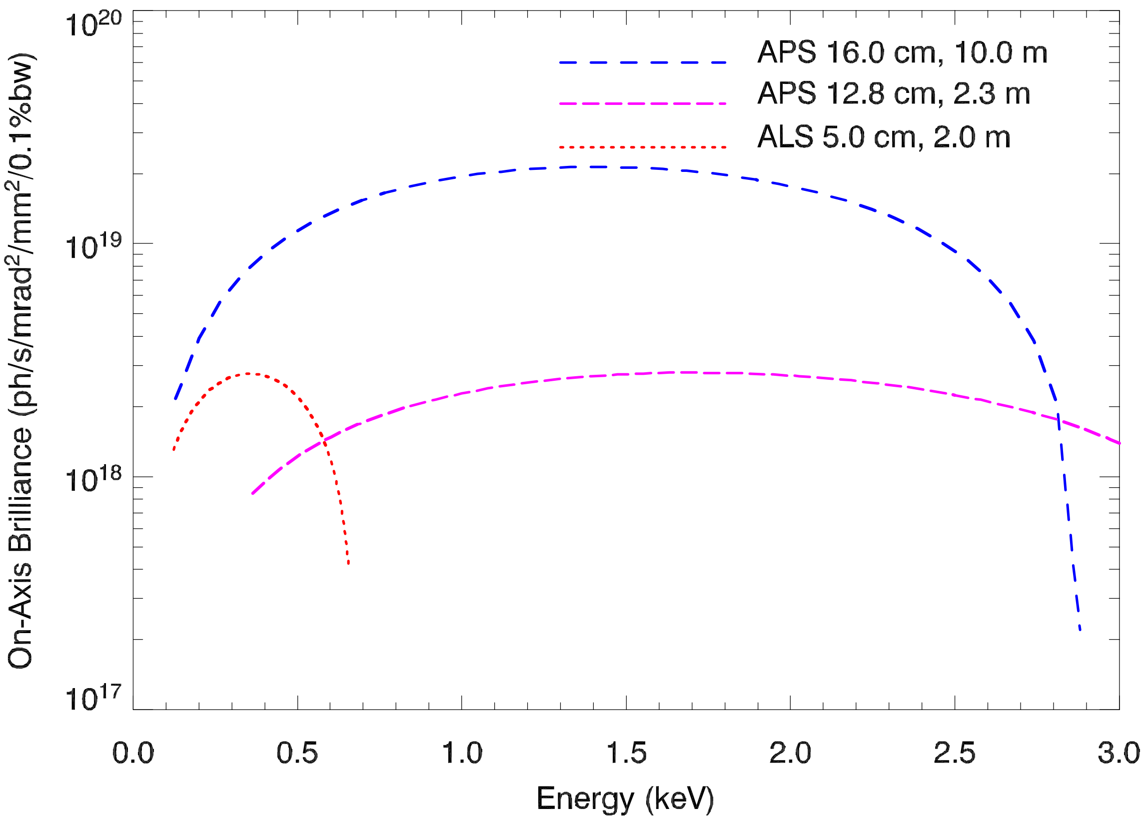

Advantages of high energy rings:

- Low emittance
- High beam stability
- Large energy tunability

⇒ **Superior performance**

APS (7 GeV, 100 mA):10 m long straight section, λ =16.0 cm, N = 62
APS (7 GeV, 100 mA):5 m long straight section, λ =12.8 cm, N = 18 (current device)
ALS (1.9 GeV, 400 mA): 2 m long straight section, λ = 5.0 cm, N = 37

Polarization-dependent spectroscopy

Helicity dependent X-ray emission provides information concerning spin polarized density of bulk occupied states

Photoemission Microscopy

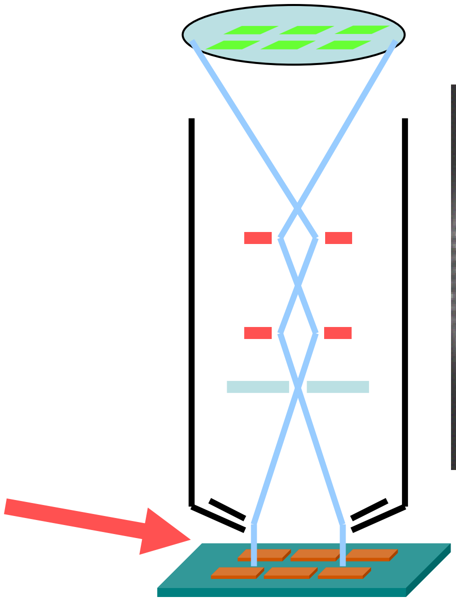

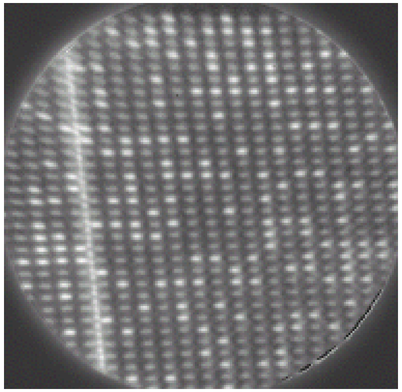

Spatial resolution target of 2 nm

- Magnetic contrast:
  - Domain imaging
  - Ground states in nanoscale systems
  - Interactions in particle arrays
  - Finite size effects
- Chemical contrast
  - Self-assembled systems
  - Segregation
  - Local electronic structure
  - Buried layers (~5 nm)
- Soft x-ray advantages:
  - High magnetic contrast
  - Access to TM, RE, semiconductors

Nano-Focusing of X-ray Beams

Brilliance = Radiated Power /0.1%BW / Unit Area / Unit Solid Angle at the Source

Brilliance is a conserved quantity in perfect optical systems
Useful in designing beamlines and synchrotron radiation experiments which involve focusing to small areas.

$$\Delta A_s \cdot \Delta\Omega_s = \Delta A_i \cdot \Delta\Omega_i$$

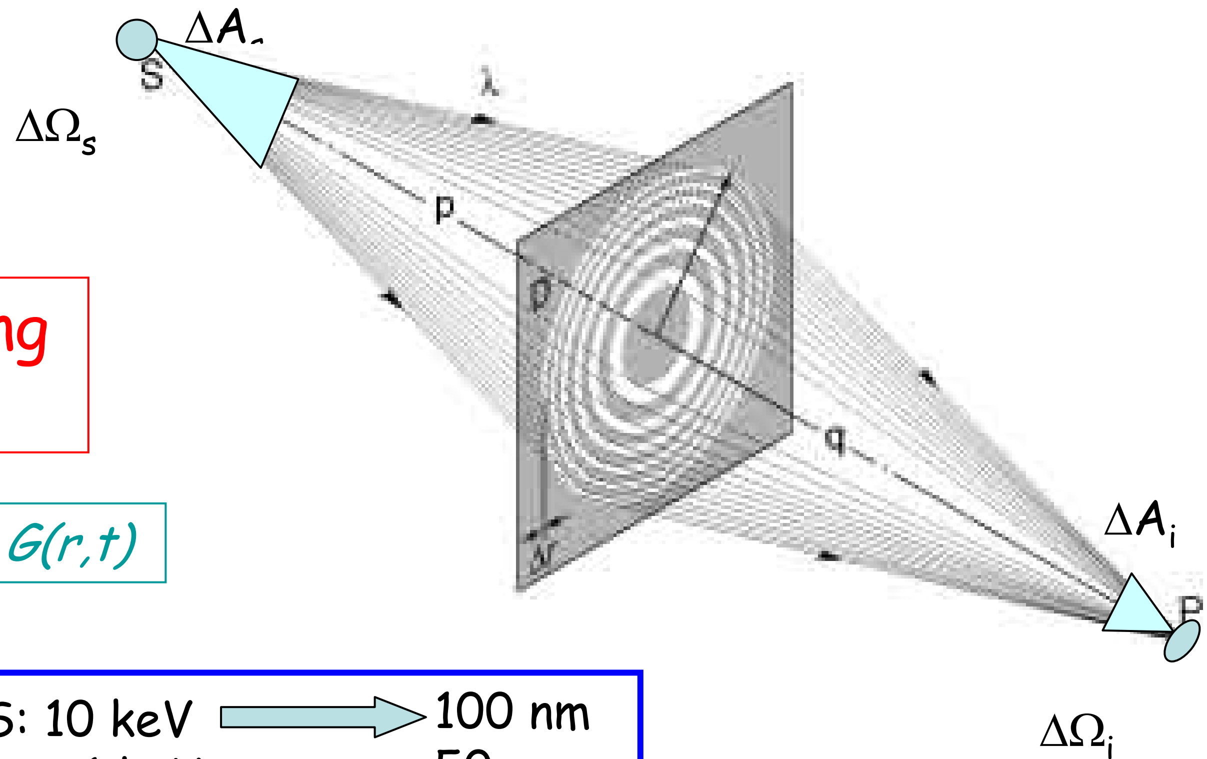

Zone Plates as Focusing Elements

Measuring Directly G(r,t)

Routine Focal Size at APS: 10 keV → 100 nm
1 keV → 50 nm

Tools for Nanoscience

- Nanoprobe
  - Scan real and reciprocal space in nanovolumes
- Adaptive optics with feedback
- Multi-parameter “smart” scans

Hard X-ray Nanoprobe

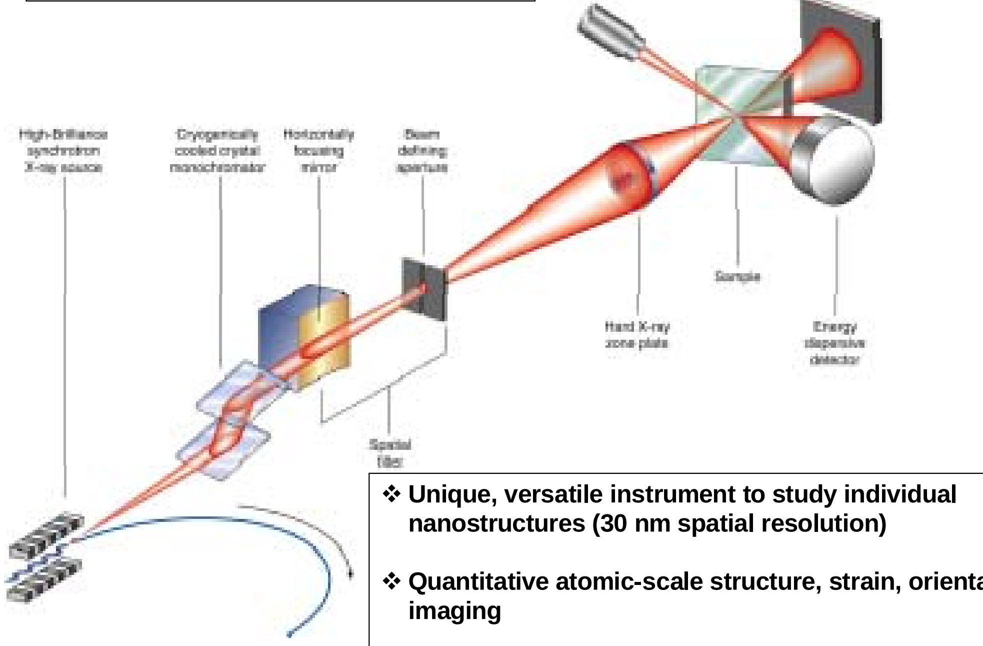

- ❖ **Unique, versatile instrument to study individual nanostructures (30 nm spatial resolution)**
- ❖ **Quantitative atomic-scale structure, strain, orientation imaging**
- ❖ **Sensitive trace element and chemical state analysis**
- ❖ **Ability to penetrate overlayers, environments, fields**

High-resolution elemental maps of a 12 μm x 12 μm area of a single nucleus containing 3.6×10^6 nanoparticles

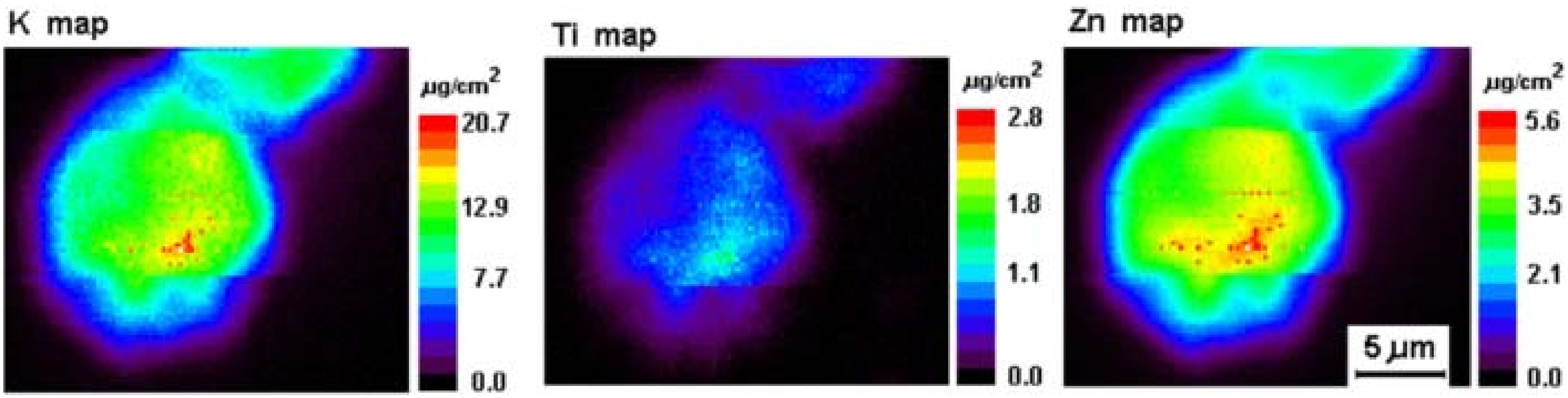

Nano-composites are introduced into cells using standard transfection methods and translocated into the cell nuclei. X-ray micro-fluorescence is crucial in quantifying the success rate of transfection and revealing the intracellular distribution of the nano-composites.

G. Woloschak et al, Nature, 2003

Transverse Coherent Flux from an Undulator

If $\varepsilon_x \cdot \varepsilon_y \sim (\lambda / 4\pi)^2$

F_c (ph/s/0.1%BW) = 1.0 $^{-8}$ x [brightness] x [λ(Å)/2] ^{2}

APS Undulator A: $F_c \sim 10^{11}$ ph/s/0.1%BW

What do you measure with coherent X-rays? F(Q,t)

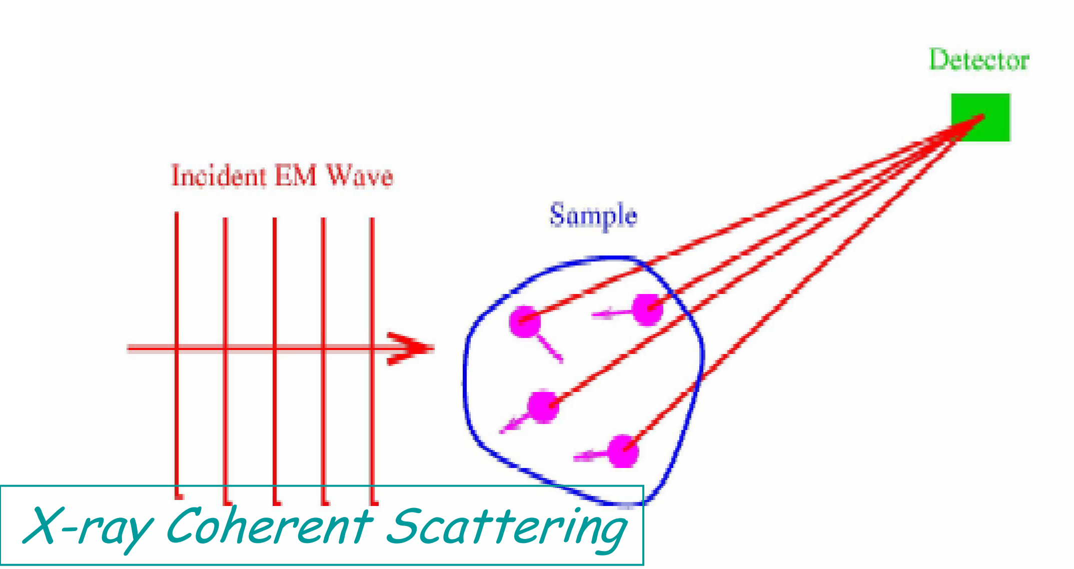

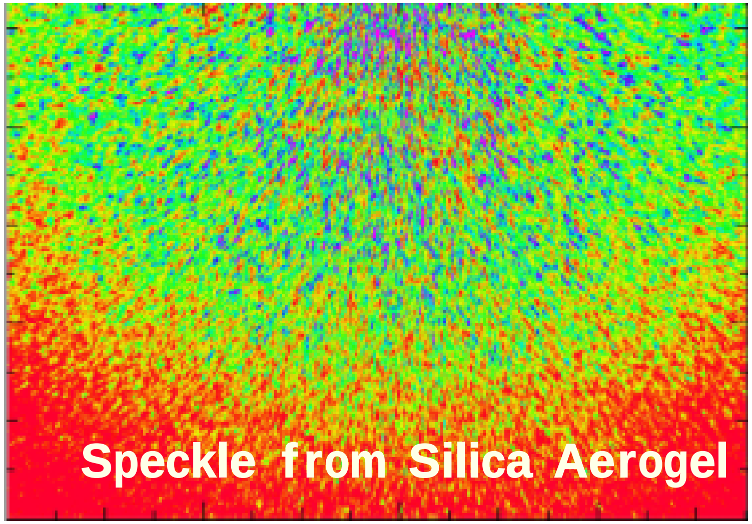

Time Autocorrelation of a Speckle Intensity

$$g_2(t) = 1 + \beta \{ F(Q,t)/F(Q,0)\}^2$$

where β is the speckle contrast

STUDIES OF INSECT RESPIRATION USING PHASE-ENHANCED, TIME-RESOLVED X-RAY IMAGING

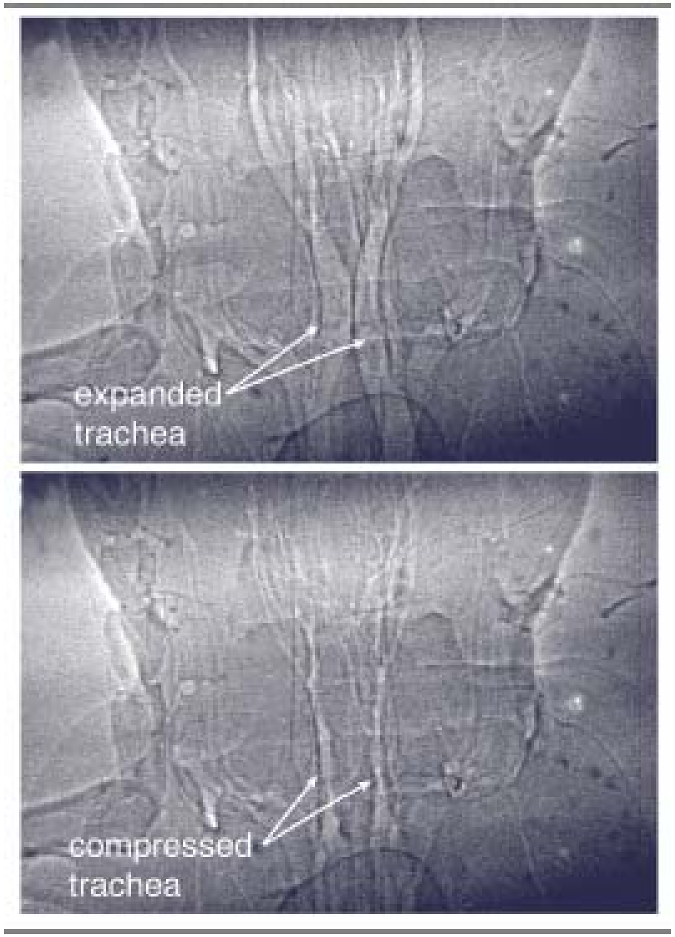

M.W. Westneat et al. Science **299**, 558-560 (24 January 2003).

Coherent X-ray Diffractive Imaging

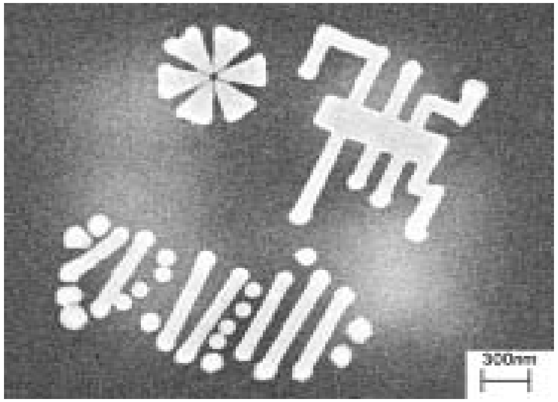

(a) **A SEM image of a double-layered sample made of Ni (~2.7 x 2.5 x 1 μm³)**

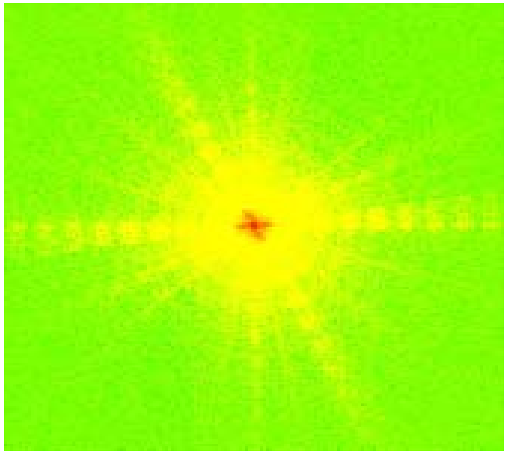

(b) **A coherent diffraction pattern from (*a*) (the resolution at the edge is 8 nm)**

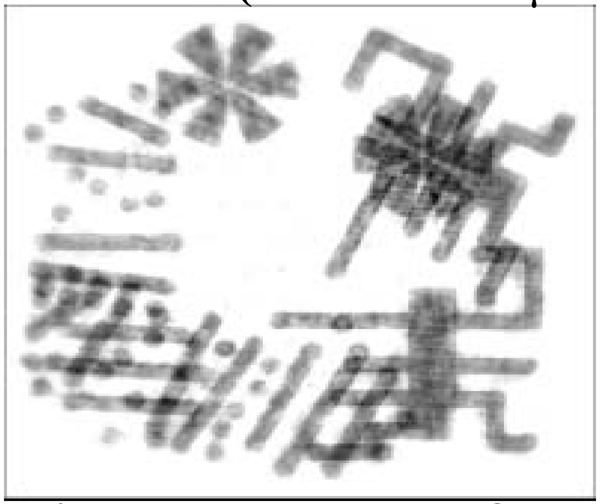

(c) **An image reconstructed from *(b)***

J. Miao et al., Phys. Rev. Lett. 89, 088303 (2002).

The Reconstructed 3D structure

The reconstructed top pattern

The reconstructed bottom pattern

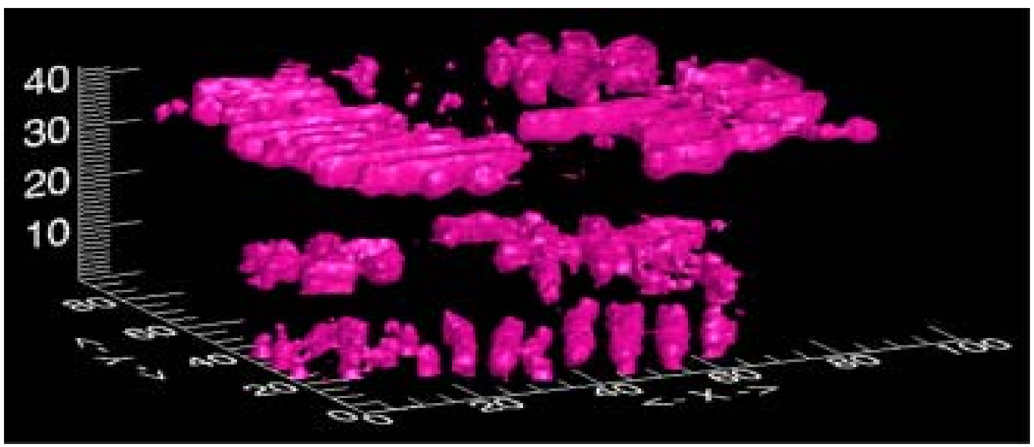

An iso-surface rendering of the reconstructed 3D structure

Inelastic X-ray Scattering Kinematics

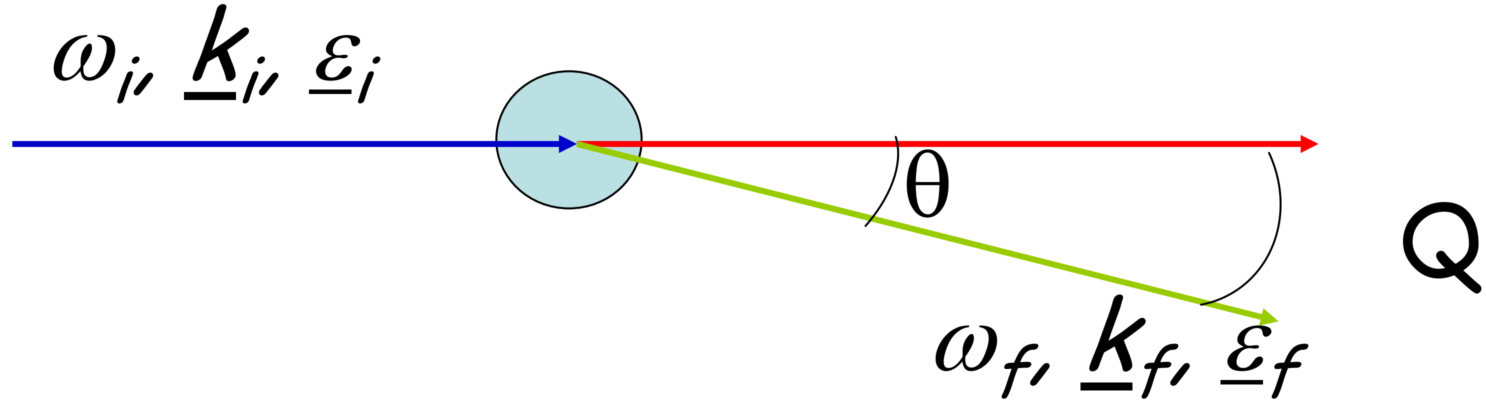

$$\underline{Q} = \underline{k}_i - \underline{k}_f$$

$$\omega = \omega_i - \omega_f$$

$$Q^2 = K_i^2 - k_f^2 - 2\,\underline{k}_i\,\underline{k}_f \cos\theta$$

Measuring Dynamic Structure Factor, S (Q, ω)

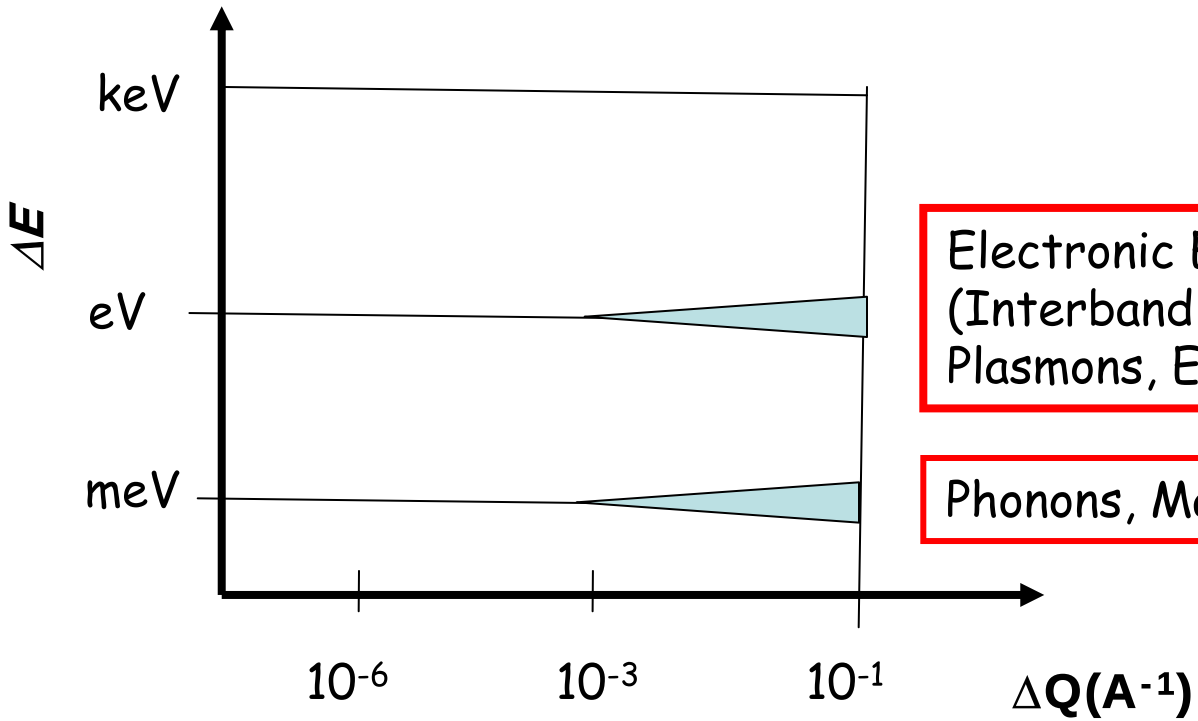

Electronic Excitations (Interband, Intraband Transitions, Plasmons, Excitons, Fluxons, etc.)

Phonons, Magnons, etc.

Brightness Driven Techniques

- Inelastic X-ray Scattering (ISX)
- Resonant Inelastic X-ray Scattering (RIXS)
- Inelastic Nuclear Resonant Scattering (INRS)

Inelastic scattering from liquid mercury at different momentum transfers

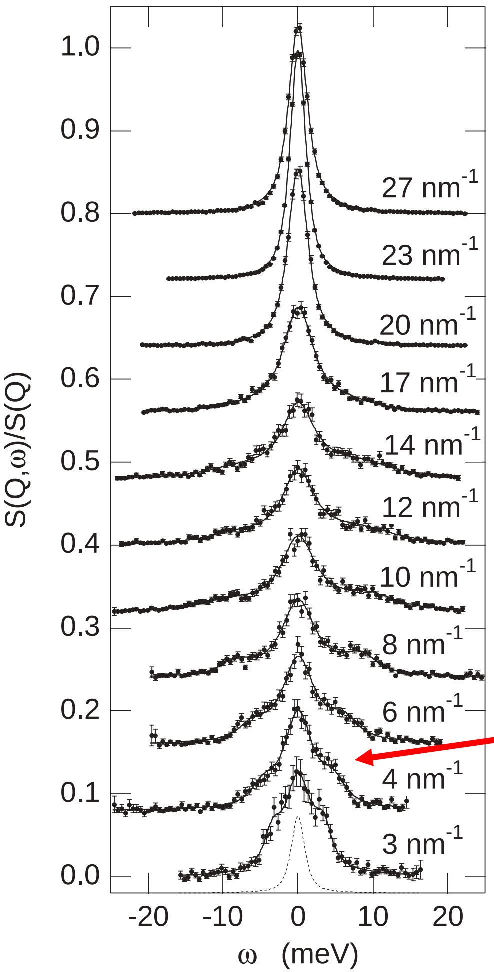

The phonon-like excitations are visible as shoulders to the central peaks at small momentum transfers.

H. Sinn, et al., Appl. Phys. A 74[Suppl.], S1648-S1650, (2002).

Resonant Inelastic X-ray Scattering (RIXS)

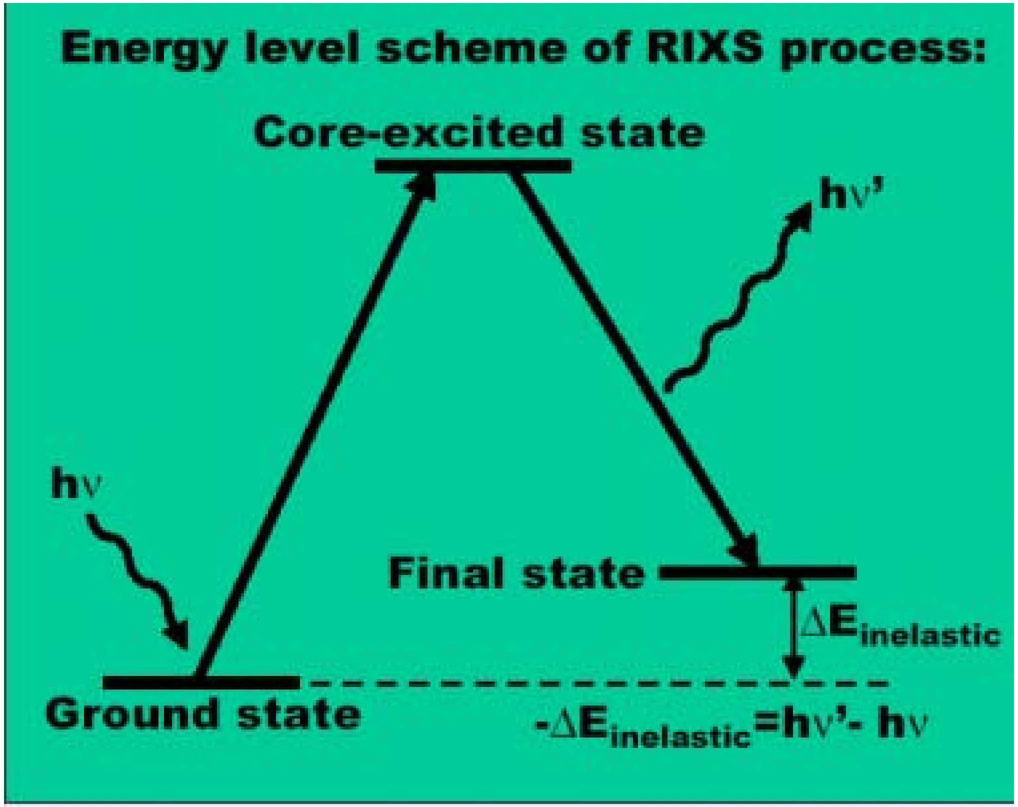

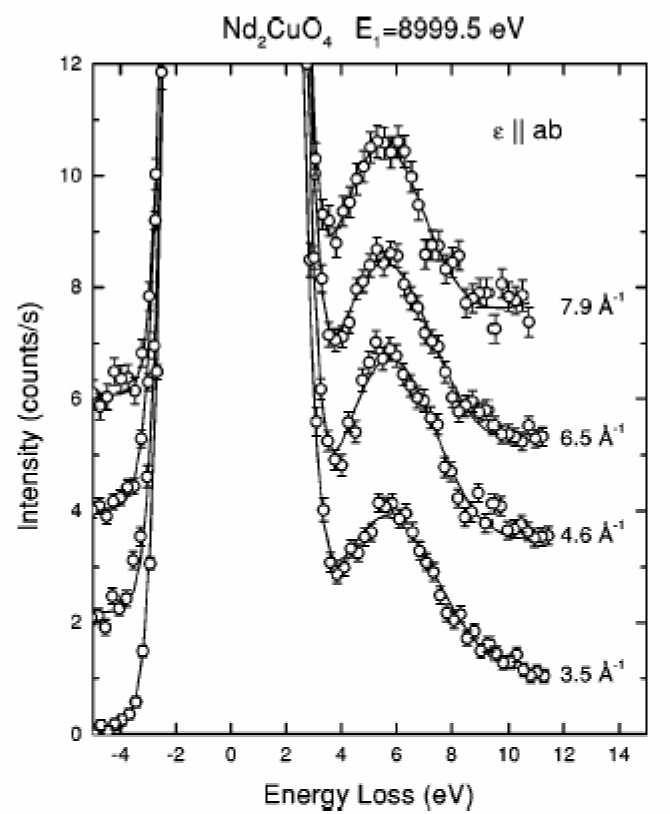

Young-June Kim, et al.,
Phys. Rev. Lett. 89, 177003-1, (2002)

- Energy-loss spectra recorded at the 1*s*/4*p* Cu resonance for different momentum transfers along the *c* axis

- The different *Q* values correspond to scattering angles of 45°, 60°, 90°, and 120°, respectively

Inelastic Nuclear Resonance Scattering in a $^{57}Fe_3BO_6$ Crystal

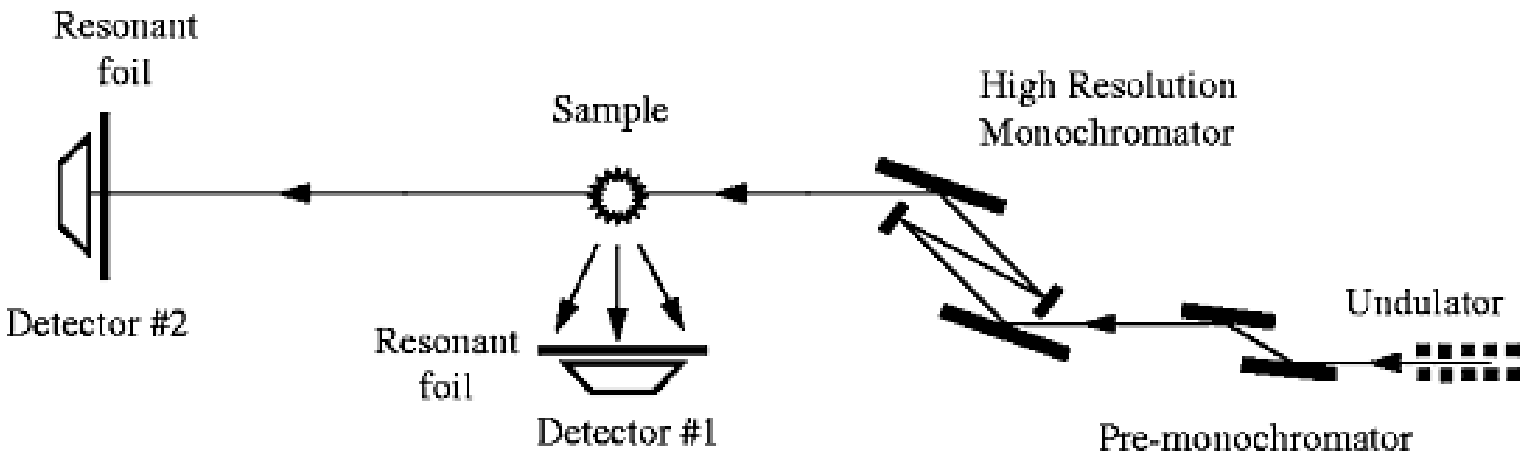

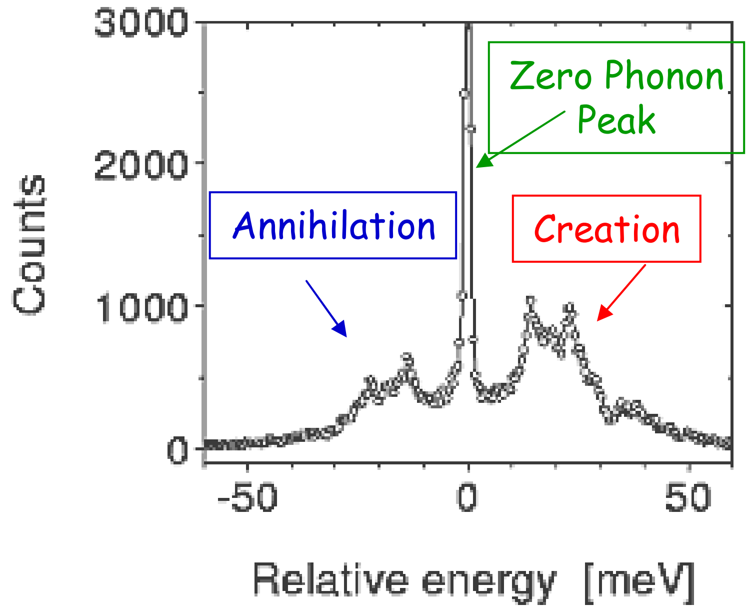

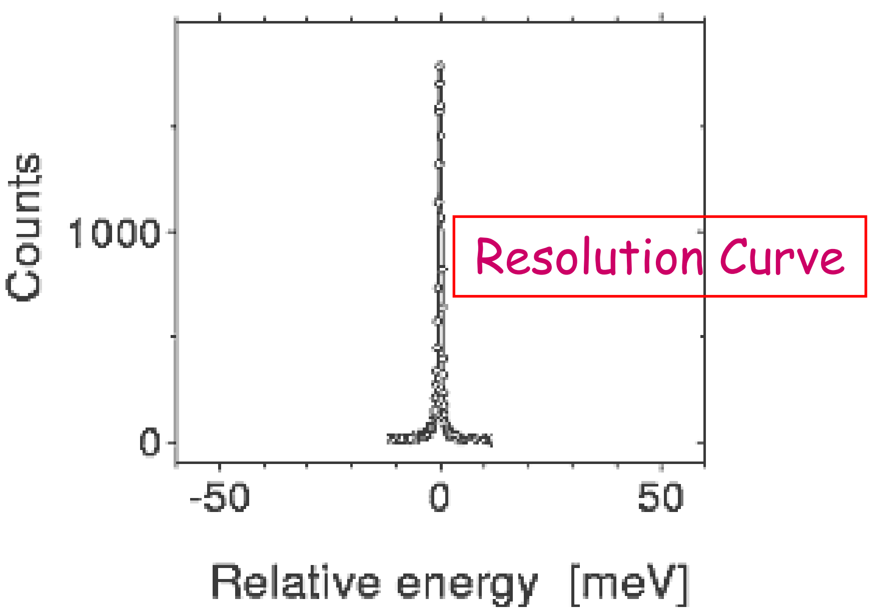

Time Domain Science

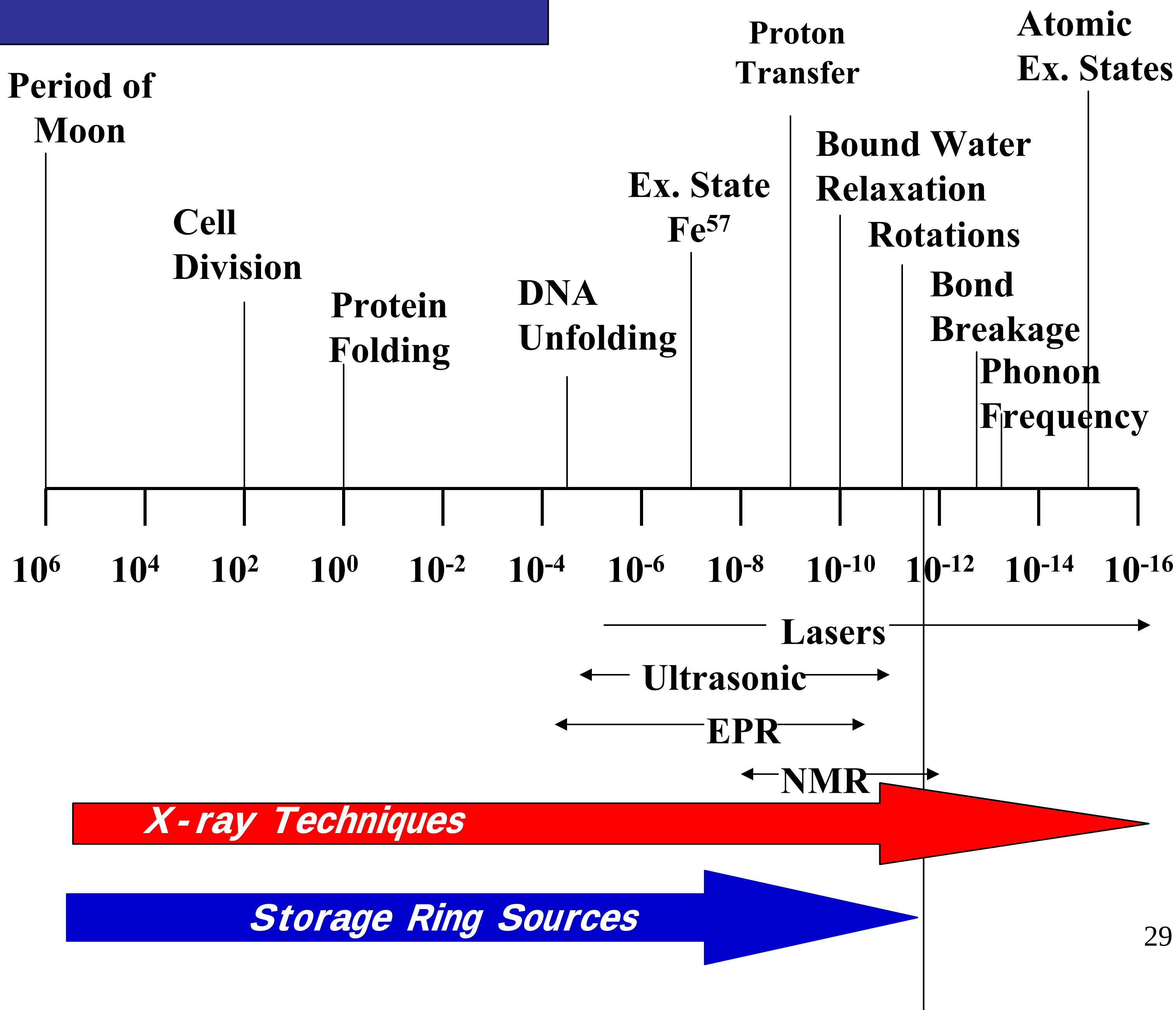

Typical Bunch Filling Patterns at APS

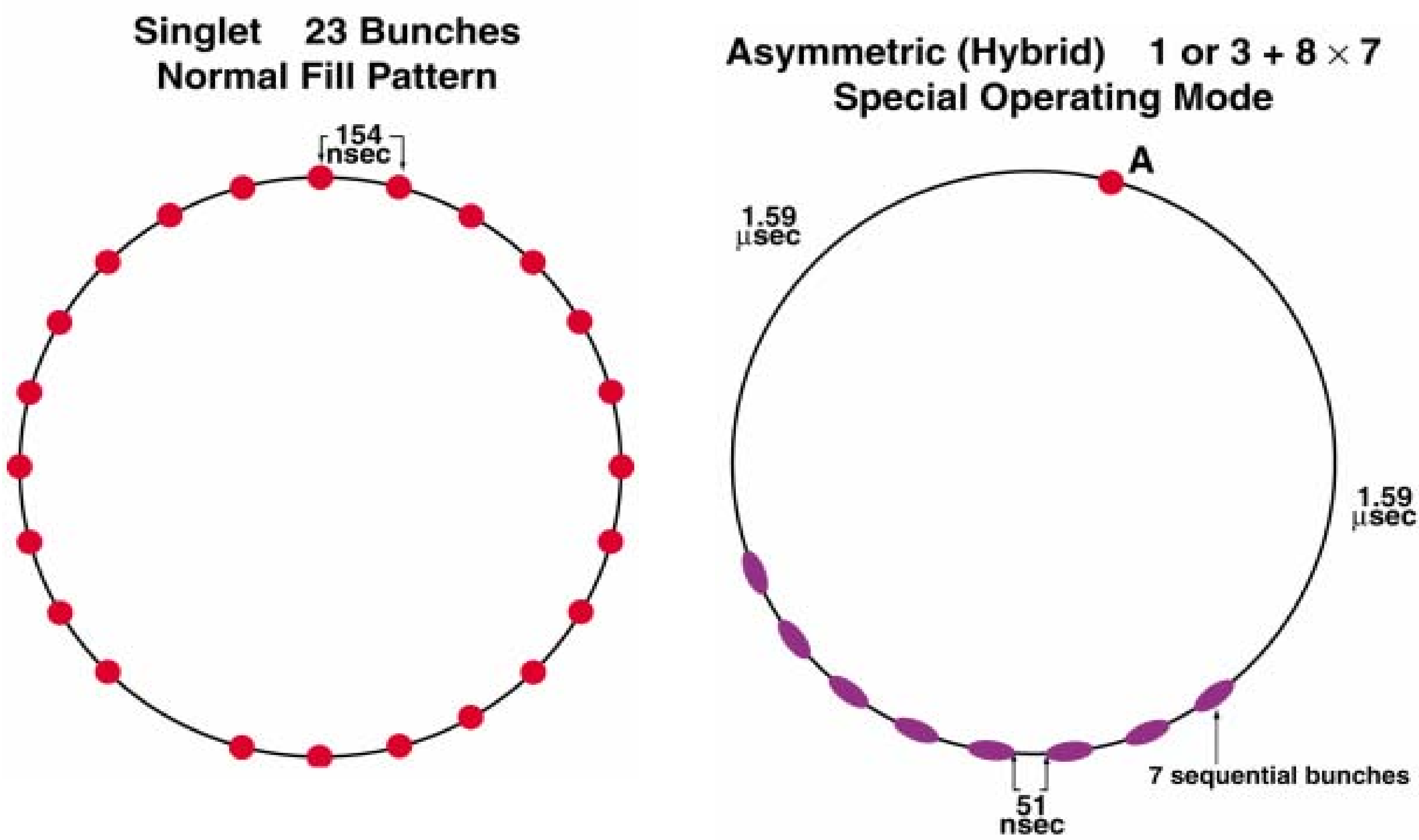

Coherent Acoustic Pulse Generated by Ultrafast Laser Excitation in InSb

D. A. Reis et al, *Phys. Rev. Lett*. 86 (2001) 3072.

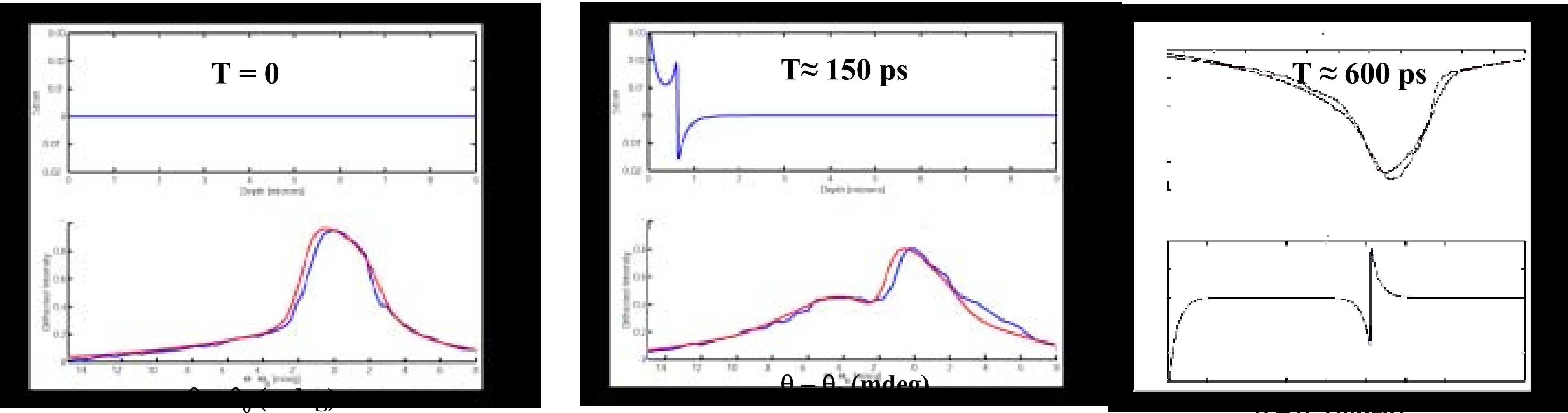

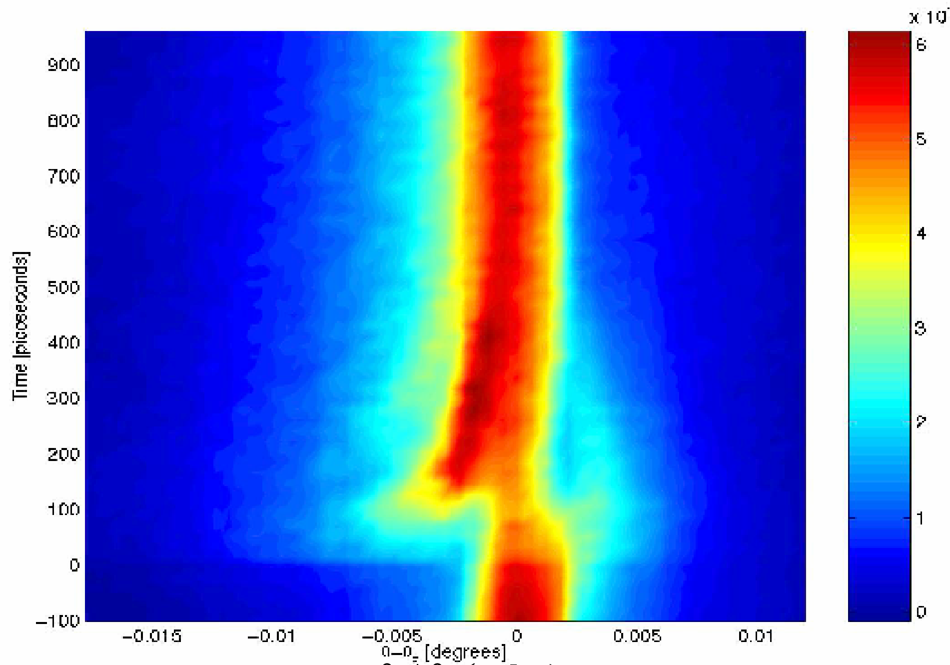

$\theta - \theta_0$ **(mdeg)**

Making a movie of chemical reactions

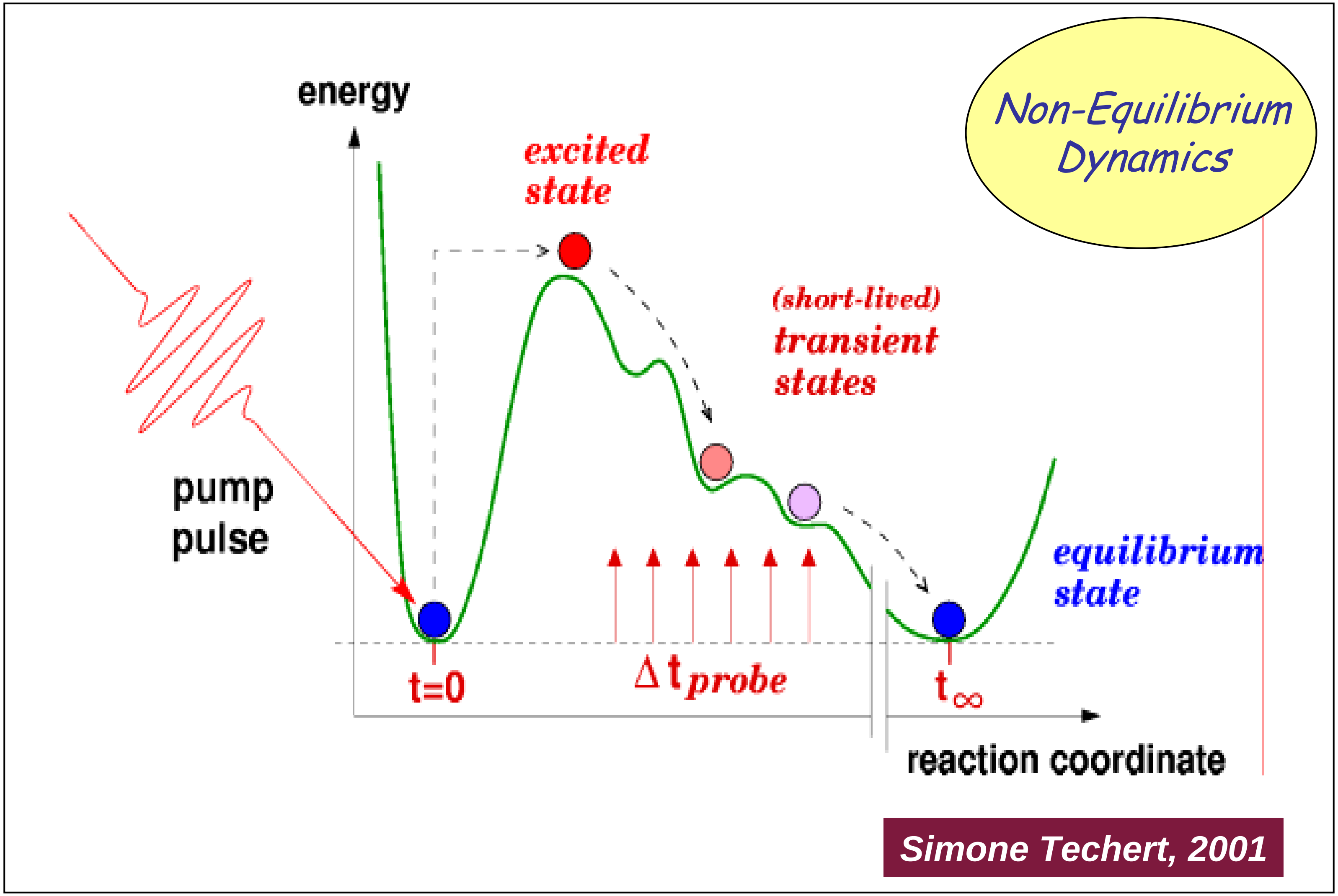

Time-resolved Crystallography

P. Coppens, I. Novozhilova and A. Kovalevsky, Chem. Rev. 102, 861-884 (2002).

If a reaction can be initiated in a crystal, simultaneously throughout the crystal, then Laue photography or x-ray spectroscopy can capture the structural changes or charge transfers at the *100 ps* (10^{-10} *s*) to *ms* (10^{-3} *s*) timescale.

Light-initiated reactions can be studied using the Laue method.

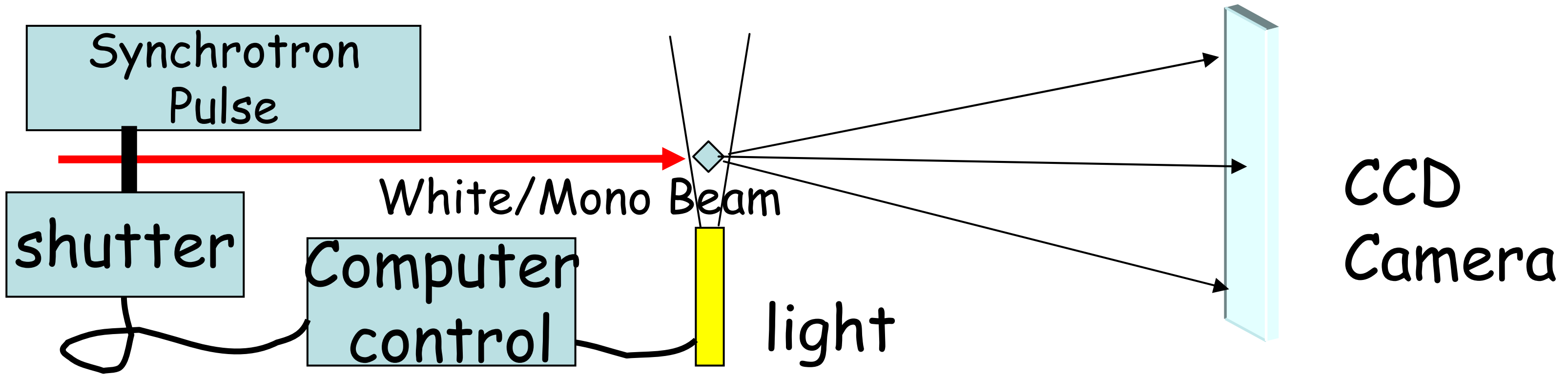

Protein Conformational Relaxation and Ligand Migration in Myoglobin: A Nanosecond to Millisecond Molecular Movie from Time-Resolved Laue X-ray Diffraction.

F(Q,t)

CO ligand is photo-dissociated by a 7.5 ns laser pulse, and the subsequent structural changes are probed by 150 ps X-ray pulses at 14 laser/X-ray delay times

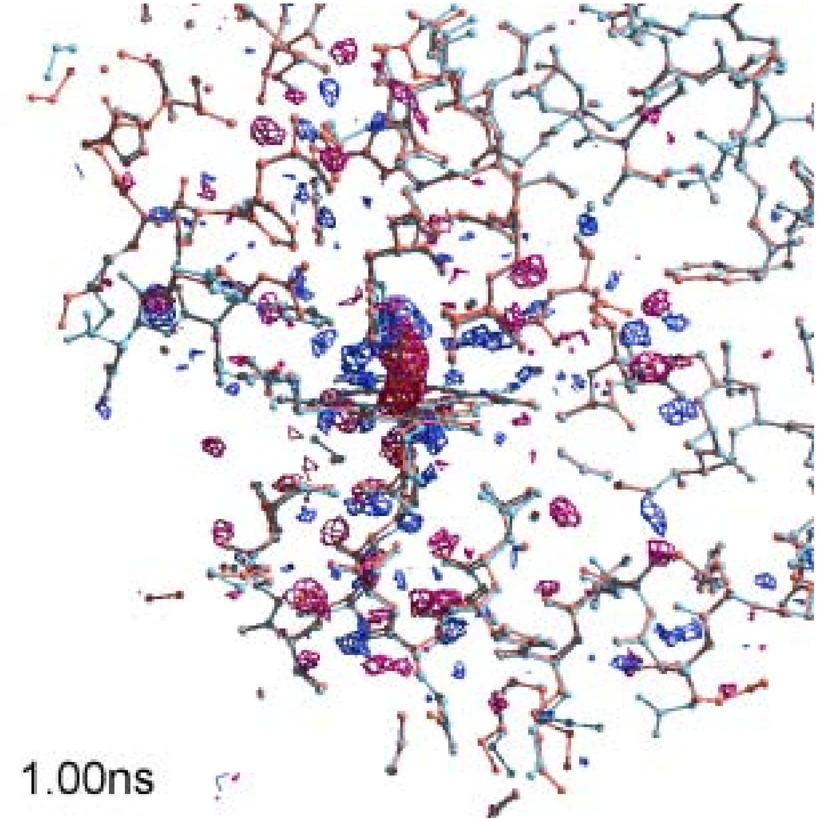

Srajer V., et al, Biochemistry 40: 13802-13815 (2001)

Light-induced Molecular Structural Rearrangements in Photochemical Reactions in Solution Studied by X-ray Absorption Spectroscopy

L. X. Chen, Angew. Chemie. Intl. Ed., (Review) **43**, 2886-2905 (2004).

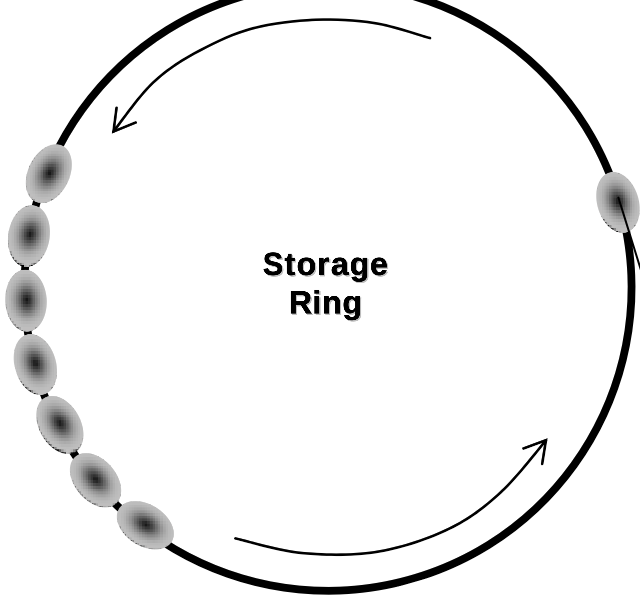

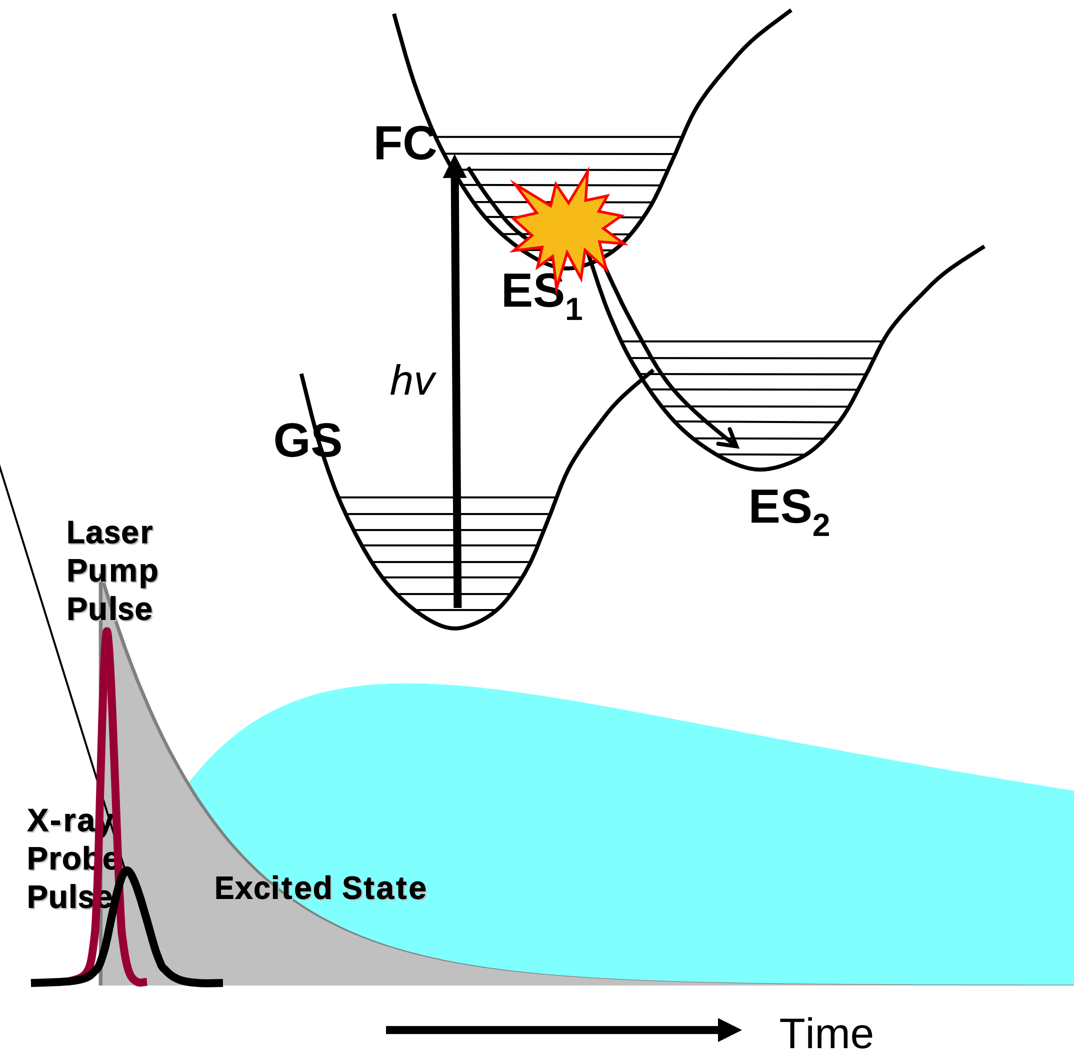

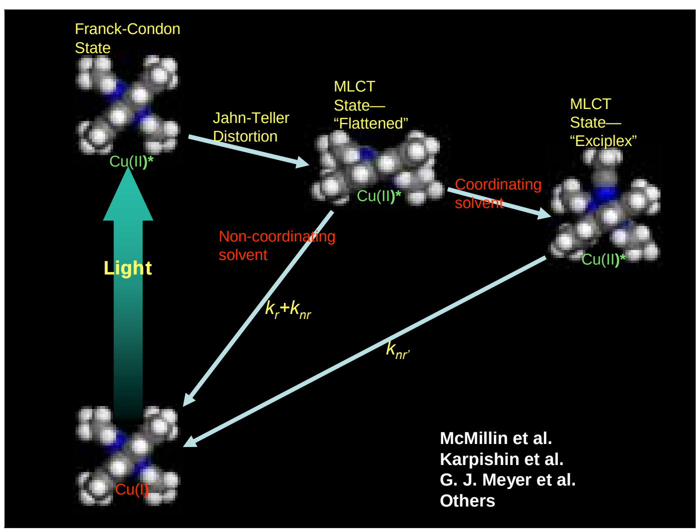

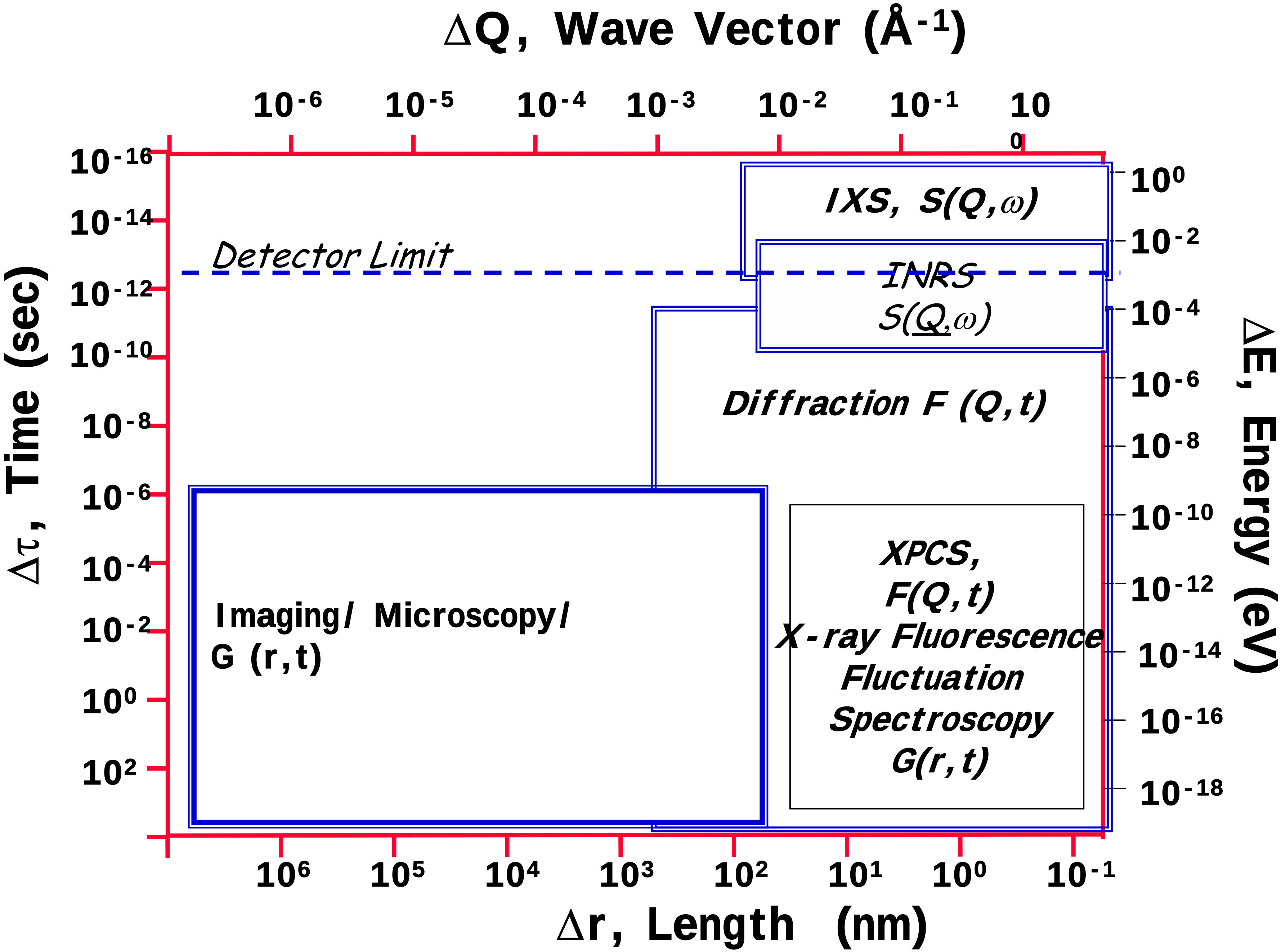
ΔQ, Wave Vector (Å-1)
10-6 10-5 10-4 10-3 10-2 10-1 100
Δτ, Time (sec)
10-16 10-14 10-12 10-10 10-8 10-6 10-4 10-2 100 102
ΔE, Energy (eV)
100 10-2 10-4 10-6 10-8 10-10 10-12 10-14 10-16 10-18
Δr, Length (nm)
106 105 104 103 102 101 100 10-1
Detector Limit
IXS, S(Q,ω)
INRS S(Q,ω)
Diffraction F (Q,t)
Imaging/ Microscopy/ G (r,t)
XPCS, F(Q,t)
X-ray Fluorescence Fluctuation Spectroscopy G(r,t)

Constant-Current or “Top-Up”Operation

Conventional Fill

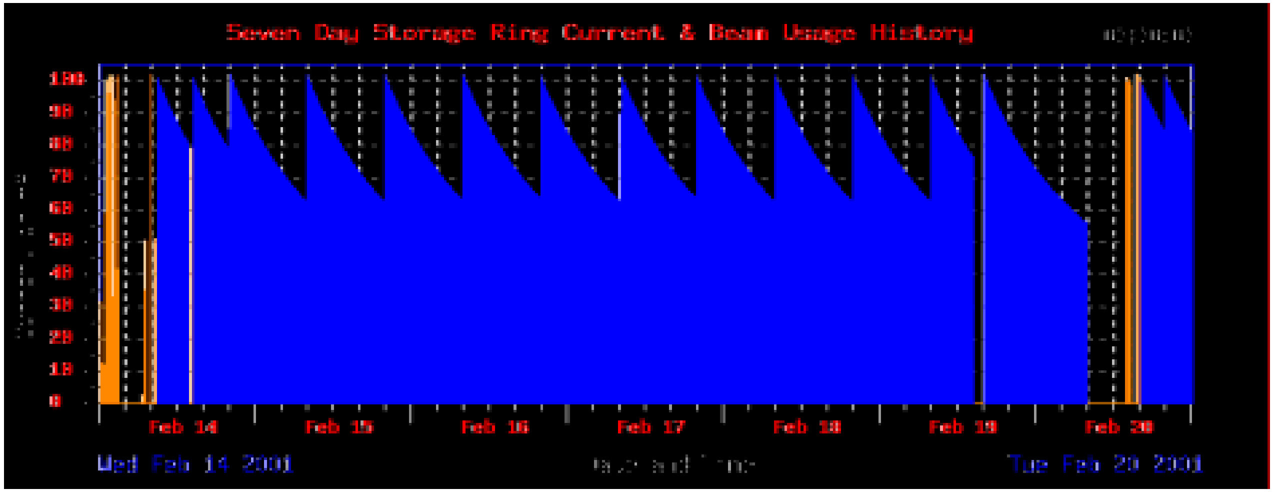

Top-Up

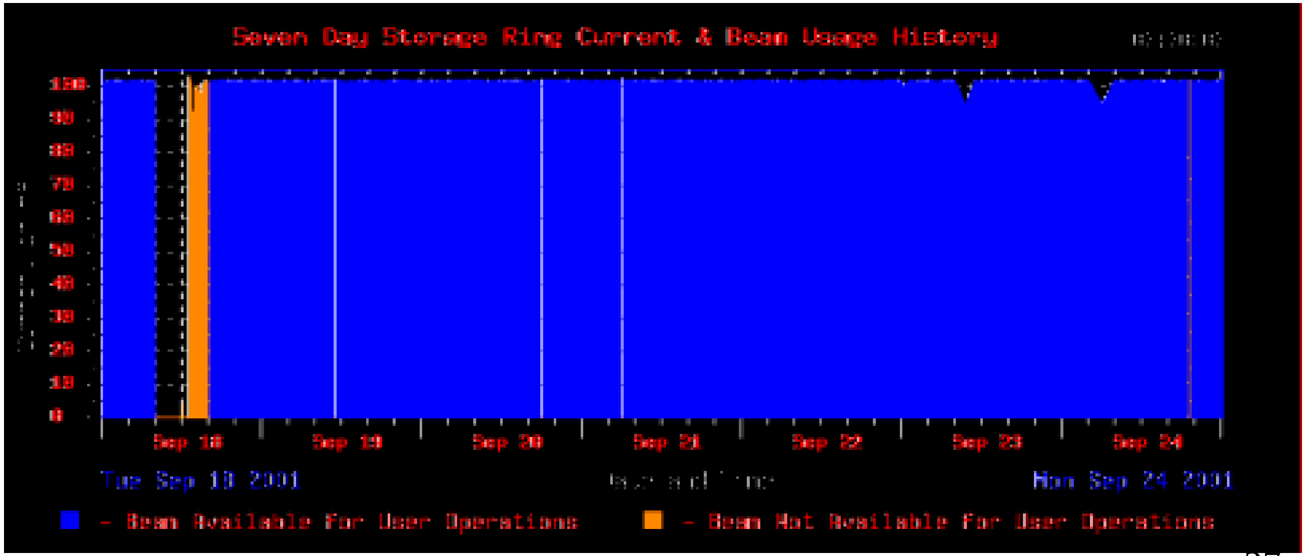

APS is first facility to begin 'Top-Up' operation starting in 1999

Maximizing APS Brilliance

Lower Emittance

$\varepsilon_x \approx 5x\ 10^{-4}\ E^2\ \varphi^3$ nm-rad

4 nm.rad → 2 nm.rad

Increased Current

100 mA

↓

300 mA

Undulators

Length: 5 m

↓

10 m

Type: Superconducting
Variable -Period

Ultimate Enhancement of APS:

Average Brightness: 10^{22-23} ph/s/0.1%BW/mm^2/mrad^2

Peak Brightness: 10^{24-25} ph/s/0.1%BW/mm^2/mrad^2

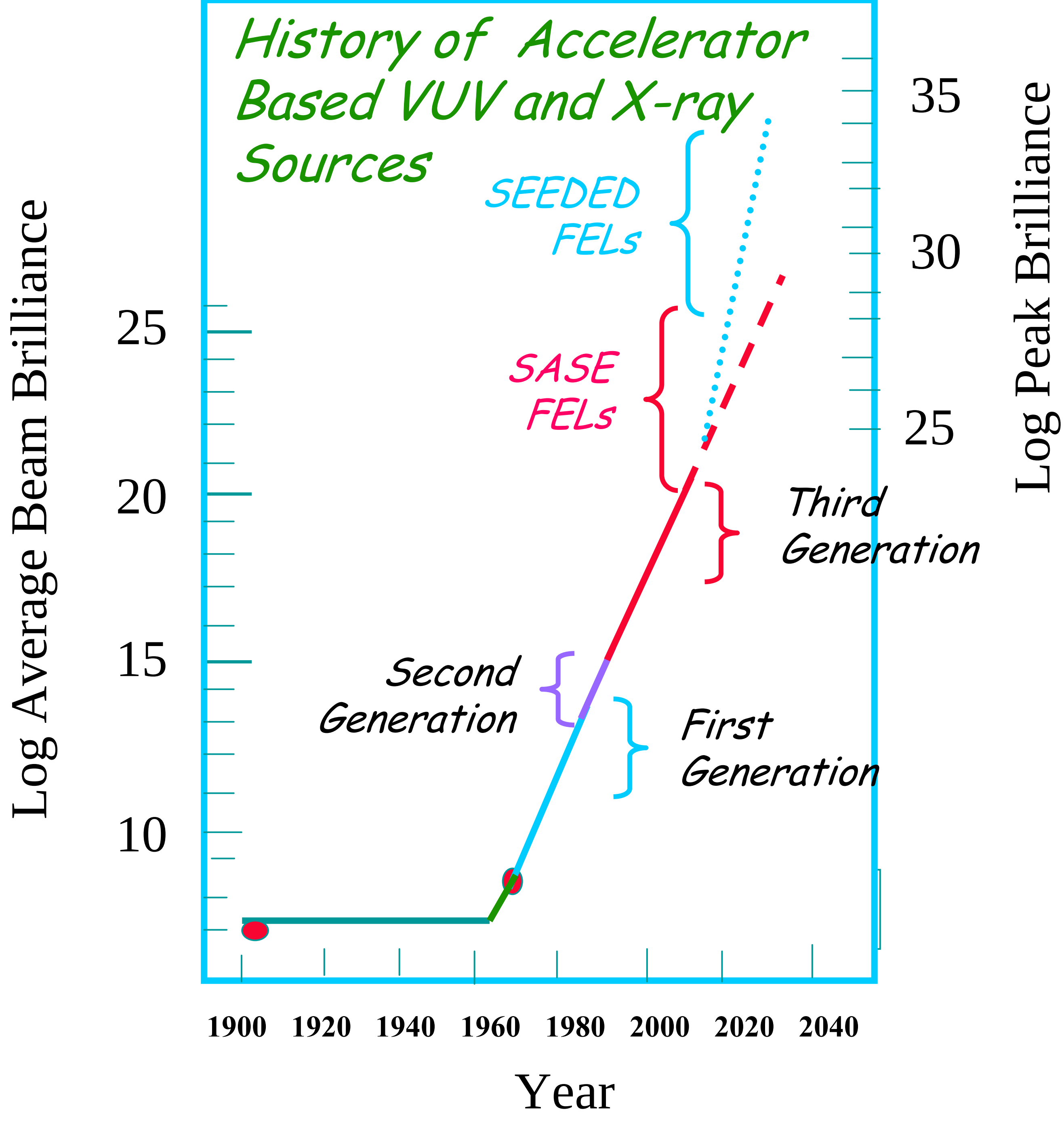
History of Accelerator Based VUV and X-ray Sources
SEEDED FELs
SASE FELs
Third Generation
Second Generation
First Generation
Log Average Beam Brilliance
Log Peak Brilliance
25
20
15
10
35
30
25
1900
1920
1940
1960
1980
2000
2020
2040
Year

APS Research Groups by Sectors and Disciplines

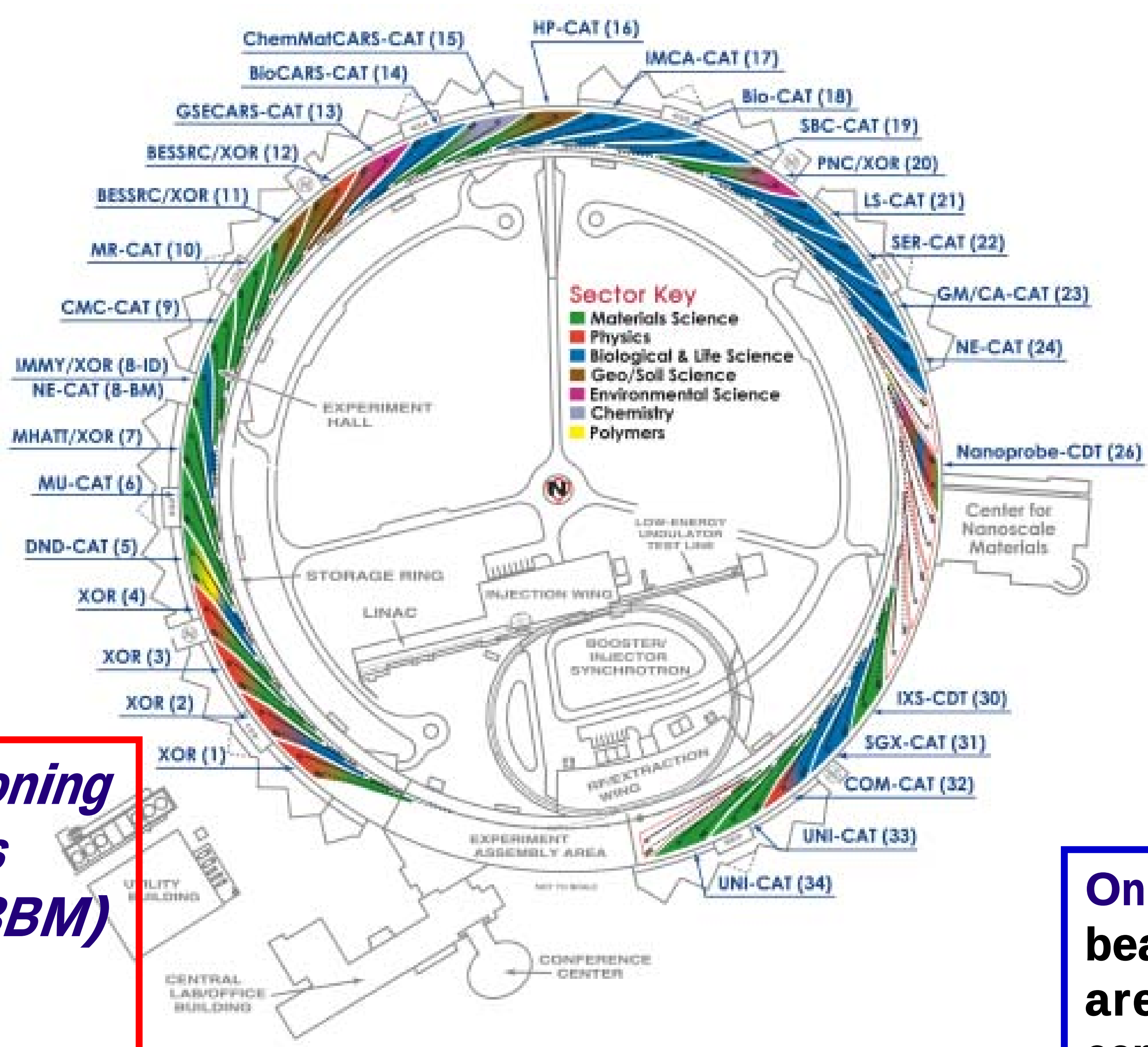

38 functioning beamports (25ID, 13BM) 68 total available

Only 4 ID beamports are not yet committed

For Beamtime at the APS:

http://www.aps.anl.gov/aps/frame_beamtime.html